Reliability analysis and updating of deteriorating systems with subset simulation

Schneider, Ronald; Thöns, Sebastian; Straub, Daniel

Published in:
Structural Safety

Link to article, DOI:
10.1016/j.strusafe.2016.09.002

Publication date:
2017

Document Version
Peer reviewed version

Manuscript accepted for publication in *Structural Safety* September 2016

Reliability analysis and updating of deteriorating systems with subset simulation

Ronald Schneider[1,*], Sebastian Thöns[2] and Daniel Straub[3]

[1]Bundesanstalt für Materialforschung und -prüfung (BAM), 7. Safety of Structures, Unter den Eichen 87, 12205 Berlin, Germany

[2]Technical University of Denmark (DTU), Department of Civil Engineering, Brovej, 2800 Kongens Lyngby, Denmark

[3]Technische Universität München (TUM), Engineering Risk Analysis Group, Arcisstr. 21, 80290 Munich, Germany

*Corresponding author: Tel.: +49-30-8104 4372 Email: ronald.schneider@bam.de

Abstract

An efficient approach to reliability analysis of deteriorating structural systems is presented, which considers stochastic dependence among element deterioration. Information on a deteriorating structure obtained through inspection or monitoring is included in the reliability assessment through Bayesian updating of the system deterioration model. The updated system reliability is then obtained through coupling the updated deterioration model with a probabilistic structural model. The underlying high-dimensional structural reliability problems are solved using subset simulation, which is an efficient and robust sampling-based algorithm suitable for such analyses. The approach is demonstrated in two case studies considering a steel frame structure and a Daniels system subjected to high-cycle fatigue.

Keywords

Structural reliability, deterioration, Bayesian analysis, inspection, monitoring, subset simulation

1 Introduction

Engineering structures are generally subjected to deterioration processes such as fatigue and corrosion, and their structural reliability may thus reduce over time. Predictions of the deterioration progress with quantitative models are uncertain due to the simplified representation of the actual deterioration phenomena, the inherent variability of the influencing parameters and limited information on those parameters. These uncertainties must be addressed when modeling

deterioration of structures (Lin and Yang 1985; Madsen et al. 1986; Melchers 1999a). Inspections and monitoring are effective means of obtaining information on the actual condition of deteriorating structures. This information should be utilized to reduce uncertainties in probabilistic models. A consistent framework for this task is provided by Bayesian analysis, in which prior probabilistic models are updated with inspection and monitoring outcomes (e.g. Tang 1973; Madsen 1987; Enright and Frangopol 1999). This approach facilitates the quantification of the effect of inspection and monitoring results on the structural reliability, and forms the basis for decisions on maintenance actions and future inspection efforts (e.g. Thoft-Christensen and Sørensen 1987; Faber et al. 2000; Moan 2005; Straub and Faber 2005).

Deterioration processes are generally correlated among structural elements within a system due to common influencing factors, such as environmental conditions and material characteristics (e.g. Moan and Song 2000; Vrouwenvelder 2004; Straub and Faber 2005; Stewart and Mullard 2007). This leads to a correlation among deterioration failures of different elements whose effect on the system reliability has to be assessed as a function of structural redundancy (Straub and Der Kiureghian 2011). Correlation among element deterioration is especially relevant when inspection and monitoring outcomes are considered in the reliability assessment (Vrouwenvelder 2004). An observation at one location within a structure contains more indirect information on the deterioration progress at another location if the correlation among element deterioration is high. For these reasons, the reliability of deteriorating structures should be analyzed and updated considering the structure as a whole.

A number of publications propose methods for computing the time-variant reliability of deteriorating structures, including works by Mori and Ellingwood (1993), Li (1995), Ciampoli (1998), Estes and Frangopol (1999), Stewart and Val (1999) and Li et al. (2015). They consider the time-dependent characteristics of both the load and resistance, but do not account for correlation among element deterioration. More recently, a number of researchers have considered modeling and updating the system deterioration state of structures, taking into account the aspect of spatial correlation among element deterioration (Moan and Song 2000; Li et al. 2004; Faber et al. 2006; Straub 2011b; Qin and Faber 2012; Maljaars and Vrouwenvelder 2014). Therein, the effect of inspections and monitoring results on the probability of either reinforcement corrosion in concrete structures or fatigue failures in steel structures is quantified using Bayesian analysis. However, the impact of deterioration on the structural reliability is not included in these works. Such integrated system reliability analyses are proposed in (Lee and Song 2014; Schneider et al. 2015; Luque and Straub 2016). Lee and Song (2014) consider sequential fatigue failures taking into account the effect of stress redistribution within a structural system. They identify critical failure sequences through a branch-and-bound scheme and iteratively compute and update bounds on the system failure probability. Luque and Straub (2016) and Schneider et al. (2015) propose the use of hierarchical Dynamic Bayesian Network (DBN) models for probabilistically representing deterioration in structural systems and for updating deterioration probabilities as well as the system

reliability with inspection and monitoring results. While they can be powerful, DBN models are rather demanding in the implementation.

To enable an integrated system reliability analysis of inspected and monitored deteriorating structures, which is computationally efficient and simple to implement, we here develop a framework using two coupled sub-models: a probabilistic system deterioration model, which considers stochastic dependence among element deterioration, and a probabilistic structural model for calculating the failure probability of the weakened system. Motivated by the work of Straub and Der Kiureghian (2011), the system deterioration state is assessed at discrete time intervals and is considered constant within each interval. Information on the deteriorating structure obtained through inspection or monitoring is included in the reliability assessment through Bayesian updating of the system deterioration model. The updated system reliability is then obtained through coupling this updated model with a probabilistic structural model. The resulting structural reliability problems are high-dimensional since they include all (correlated) deteriorating elements. To solve these problems, we apply subset simulation, which is a sampling-based algorithm that can robustly and efficiently handle problems involving a large number of random variables. The method is demonstrated in two case studies considering welded steel structures subjected to fatigue deterioration.

2 System reliability analysis of deteriorating structures

2.1 Deterioration modeling

Deterioration is modeled at the element level at discrete time steps. An element may be a structural member, a welded connection or a segment of a continuous surface (Straub and Der Kiureghian 2011). The state of deterioration of an element i at time t is represented by a random variable or random vector $D_{i,t}$. For example, in the context of reinforcement corrosion in concrete structures, $D_{i,t}$ may represent the loss of reinforcement cross section. Deterioration of all elements is influenced by a set random variables $\mathbf{X} = (X_1, \dots, X_n)$. The relationship between $\mathbf{X}$ and $D_{i,t}$ is described by a parametric deterioration model h_i, which is written in generic form as:

$$D_{i,t} = h_i(\mathbf{X}, t) \tag{1}$$

The joint probability density function (PDF) of $\mathbf{X}$ is denoted by $f_{\mathbf{X}}(\mathbf{x})$. Model uncertainties arising from a simplified representation of the actual deterioration phenomenon are included through additional random variables in $\mathbf{X}$.

All random variables describing the deterioration state of the individual elements at time t are summarized in a vector $\mathbf{D}_t = \left(D_{1,t}, \dots, D_{n_E,t}\right)$, where n_E is the number of elements considered in the system reliability analysis. This vector represents the overall deterioration state of the structural

system at time t. The relationship between the system deterioration state $\mathbf{D}_t$ and the deterioration model parameter $\mathbf{X}$ is described by a function $\mathbf{h}$ as:

$$\mathbf{D}_t = \mathbf{h}(\mathbf{X}, t) = \left(h_1(\mathbf{X}, t), \dots, h_{n_E}(\mathbf{X}, t)\right) \tag{2}$$

2.2 Modeling dependence among deterioration model parameters

Deterioration of different elements of a structural system is generally interdependent due to the spatial correlation among the uncertain parameters $\mathbf{X}$ influencing their condition. Such spatial dependencies are often due to geometrical proximity, but they mainly exist due to common factors influencing the element condition such as environmental conditions and material characteristics (Luque and Straub 2016). The aspect of spatial correlation of deterioration is especially relevant when inspection and monitoring outcomes are considered in the reliability assessment of deteriorating structures. The effect of such observations on the reliability strongly depends on the spatial correlation among the parameters $\mathbf{X}$. An observation at one location contains more indirect information on the deterioration progress at another location if the correlation among the parameters $\mathbf{X}$ is high.

There is only limited information available on modeling statistical dependence of deterioration in structural systems (e.g. Vrouwenvelder 2004; Malioka 2009; Luque et al. 2016). For example, Vrouwenvelder (2004) estimated the correlation among uncertain parameters influencing fatigue crack growth in welded connections by comparing the scatter of the parameters within one production series to the scatter in the overall population. In most applications, however, correlation among the uncertain parameters $\mathbf{X}$ has to be estimated based at least partially on engineering judgment.

Hierarchical models and random field models are commonly applied to represent spatial dependence among the uncertain parameters $\mathbf{X}$. The latter are suitable for representing parameters with inherent spatial variability (e.g. Hergenröder 1992; Stewart and Mullard 2007; Malioka 2009). The random field approach models a spatially varying parameter X as a random variable $X(z)$ at each location z, and describes the correlation structure of the different random variables $X(z)$ in terms of a suitable correlation function. Such random fields are typically discretized to enable their numerical representation (see, for example, Betz et al. 2014a). As a result, a random field of a spatially varying parameter is defined by a discrete set of correlated random variables, which are part of $\mathbf{X}$. The joint distribution of the variables in a random field is commonly represented by the Nataf model, also known as the Gaussian copula (Liu and Der Kiureghian 1986).

Hierarchical models may be applied if common influencing factors can be modeled explicitly (e.g. Maes and Dann 2007; Luque et al. 2016). Such models represent correlation among random variables by defining different levels. The random variables within one level are linked through

common influencing factors, which are modeled as random variables at a higher level in the hierarchy. The random variables at the highest level are often called hyper-parameters (see, for example, Maes and Dann 2007). The additional random variables representing common influencing factors in a hierarchical model are included in $\mathbf{X}$. The probability distributions of the random variables in each level are defined conditional on the random variables at the next higher level in the hierarchy. Such a hierarchical dependence structure among the variables in $\mathbf{X}$ can be implemented through the Rosenblatt transformation (Hohenbichler and Rackwitz 1981).

In many instances common influencing factors can, however, not be modeled explicitly. Instead, statistical dependence among the variables in $\mathbf{X}$ is often represented by correlation coefficients. As an example, statistical dependence of fatigue deterioration among welded connections due to common fabrication quality may be modeled by defining a correlation coefficient between the initial crack sizes at different hotspots (Vrouwenvelder 2004). In this case, the Nataf model can be applied to model the joint distribution of the correlated deterioration model parameters.

Parameters influencing deterioration can also be time variant. Such parameters are ideally modeled by stochastic processes (see, for example, Lin and Yang 1985; Straub and Faber 2007; Altamura and Straub 2014). Similar to a random field, a stochastic process represents a time-varying parameter X as a random variable $X(t)$ at each time t, and describes the correlation among the random variables $X(t)$ through a suitable correlation function. Continuous-time stochastic processes are discretized to facilitate their numerical representation. The resulting set of correlated random variables is included in $\mathbf{X}$. The joint distribution of the variables in a stochastic process may be represented by the Nataf model. In case a stochastic process has the Markov property, the Rosenblatt transformation may be applied (see, for example, Altamura and Straub 2014).

2.3 Prior system failure probability

The system failure probability is assessed conditional on the system deterioration state $\mathbf{D}_t$. In agreement with Straub and Der Kiureghian (2011), the deterioration state of a structure is considered constant over a period Δt. The value of Δt depends on how fast deterioration progresses and on the lifetime of the structure. In most applications, a good choice is $\Delta t = 1$ year, which is short compared to the typical lifetime of structural systems. Conservatively, the system deterioration state in the period $[t - \Delta t, t]$ is set equal to the state at time t, $\mathbf{D}_t$. The relationship between the system deterioration state $\mathbf{D}_t$ and the deterioration model parameters $\mathbf{X}$ is described by Equation (2). Let F_t denote the event of system failure in the period $[t - \Delta t, t]$. The probability of this event conditional on a realization of the deterioration model parameters $\mathbf{x}$ is written as:

$$p_F(\mathbf{x}, t) = \Pr(F_t|\mathbf{X} = \mathbf{x}) = \Pr\big(F_t|\mathbf{D}_t = \mathbf{h}(\mathbf{x}, t)\big) \tag{3}$$

To include the uncertainty in the deterioration model parameters, the total probability theorem is applied. The overall probability of system failure in the reference period $[t - \Delta t, t]$ is:

$$\Pr(F_t) = \int_{\boldsymbol{D}_\mathbf{X}} \Pr(F_t|\mathbf{X}=\mathbf{x})\, f_\mathbf{X}(\mathbf{x})\, d\mathbf{x} = \int_{\boldsymbol{D}_\mathbf{X}} p_F(\mathbf{x},t)\, f_\mathbf{X}(\mathbf{x})\, d\mathbf{x} \tag{4}$$

where $\boldsymbol{D}_\mathbf{X}$ denotes the domain of definition of $\mathbf{X}$. The total-probability-form of the structural reliability problem is advantageous when random variables not contained in $\mathbf{X}$ also influence the event of system failure F_t (Straub and Der Kiureghian 2010). Such random variables are considered in the computation of $p_F(\mathbf{x},t)$. By defining the problem in this form, the deterioration model is decoupled from the structural model.

The conditional system failure probability $p_F(\mathbf{x},t) = \Pr\big(F_t|\mathbf{D}_t = \mathbf{h}(\mathbf{x},t)\big)$ is computed by performing system reliability analyses of the damaged structure. To this end, the structural model is defined with element properties according to the system deterioration state $\mathbf{D}_t = \mathbf{h}(\mathbf{x},t)$. Random variables influencing the system reliability which are not contained in $\mathbf{X}$ are typically load and resistance parameters. While resistance parameters, such as material strengths and structural dimensions, are usually modeled as time-invariant random variables, load parameters are mostly stochastic processes. However, it is typically sufficient to represent the load process by its extreme value distribution for the reference period $[t-\Delta t, t]$ (Melchers 1999b; Straub and Der Kiureghian 2011). The computation of $p_F(\mathbf{x},t)$ then reduces to a time-invariant reliability analysis of the weakened system. This approach leads to an accurate solution if the load process is ergodic and the maximum loads in two different time periods are statistically independent of each other. This holds at least approximately for most relevant applications.

Equation (4) can be transformed into a component reliability problem following Wen and Chen (1987). To this end, we introduce an auxiliary standard uniform random variable P with PDF $f_P(p) = 1$ and cumulative distribution function (CDF) $F_P(p) = p$. We now note that the following identity holds:

$$p_F(\mathbf{x},t) = F_P\big(p_F(\mathbf{x},t)\big) = \Pr\big(P \le p_F(\mathbf{x},t)\big) \tag{5}$$

The right hand side of Equation (5) corresponds to a component reliability problem with limit-state function:

$$g_F(\mathbf{x},p,t) = p - p_F(\mathbf{x},t) \tag{6}$$

The limit-state function $g_F(\mathbf{x},p,t)$ describes a domain $\Omega_F(t)$ in the augmented outcome space of $\mathbf{X}$ and P as $\Omega_F(t) = \{(\mathbf{x},p) : g_F(\mathbf{x},p,t) \le 0\}$. The conditional probability $p_F(\mathbf{x},t)$ can now be expressed as:

$$p_F(\mathbf{x},t) = \int_{p\in\Omega_F(t)} f_P(p)\, dp = \int_0^1 I(g_F(\mathbf{x},p,t) \le 0)\, f_P(p)\, dp \tag{7}$$

where $I(\cdot)$ is the indicator function: $I(\cdot) = 1$ if the condition $(\cdot)$ is true and $I(\cdot) = 0$ otherwise. Inserting Equation (7) into Equation (4) gives:

$$\begin{aligned}\Pr(F_t) &= \int_{\boldsymbol{D}_\mathbf{X}} \left[\int_0^1 I(g_F(\mathbf{x}, p, t) \le 0)\, f_P(p)\, dp \right] f_\mathbf{X}(\mathbf{x})\, d\mathbf{x} \\ &= \int_{\boldsymbol{D}_\mathbf{X}} \int_0^1 I(g_F(\mathbf{x}, p, t) \le 0)\, f_\mathbf{X}(\mathbf{x})\, f_P(p)\, d\mathbf{x}\, dp \\ &= \int_{(\mathbf{x},p)\in\Omega_F(t)} f_\mathbf{X}(\mathbf{x})\, f_P(p)\, d\mathbf{x}\, dp \end{aligned} \tag{8}$$

Equation (8) can be solved using structural reliability methods (e.g. Ditlevsen and Madsen 1996). As discussed earlier, such a calculation requires the computation of the conditional system failure probability $p_F(\mathbf{x}, t) = \Pr\big(F_t | \mathbf{D}_t = \mathbf{h}(\mathbf{x}, t)\big)$, which can be determined using system reliability analysis methods (see, for example, Hohenbichler and Rackwitz 1983; Ditlevsen and Bjerager 1986; Thoft-Christensen and Murotsu 1986; Naess et al. 2009; Song and Kang 2009). If the number of distinct system deterioration states $\mathbf{D}_t = \mathbf{d}_t$ is limited, $\Pr(F_t | \mathbf{D}_t = \mathbf{d}_t)$ may be pre-computed for all $\mathbf{D}_t = \mathbf{d}_t$. If this is not possible, $\Pr(F_t | \mathbf{D}_t = \mathbf{d}_t)$ has to be computed during the evaluation of Equation (8). The computation of $\Pr(F_t | \mathbf{D}_t = \mathbf{d}_t)$ is discussed in more detail in Section 7.

For the purpose of applying structural reliability methods, it is convenient to transform the reliability problem defined in Equation (8) to standard normal space. To this end, the auxiliary random variable P and the deterioration model parameters $\mathbf{X}$ are transformed to independent standard normal random variables $\mathbf{U} = (U_0, U_1, \dots, U_n)$. P and $\mathbf{X}$ are independent and can be transformed separately. The inverse transformation from $\mathbf{U}$ to P and $\mathbf{X}$ is as follows (see also Straub and Papaioannou 2015b):

$$P = \Phi(U_0) \tag{9}$$

where $\Phi(\cdot)$ is the standard normal CDF, and

$$\mathbf{X} = \mathbf{T}^{-1}(U_1, \dots, U_n) \tag{10}$$

$\mathbf{T}(\cdot)$ is a probability preserving one-to-one mapping from the original outcome space of $\mathbf{X}$ to the standard normal space for which the Rosenblatt transformation (Hohenbichler and Rackwitz 1981) or the Nataf transformation (Liu and Der Kiureghian 1986) can be applied (see also Section 2.2).

The limit-state function g_F is now transformed to $\mathbf{U}$-space as:

$$G_F(\mathbf{u}, t) = u_0 - \Phi^{-1}\big(p_F(\mathbf{T}^{-1}(u_1, \dots, u_n), t)\big) \tag{11}$$

G_F describes the domain $\Omega_F^U(t)$ in the transformed space as $\Omega_F^U(t) = \{\mathbf{u} : G_F(\mathbf{u}, t) \leq 0\}$. Therefore, the system failure probability $\Pr(F_t)$ can be expressed in **U**-space as:

$$\Pr(F_t) = \Pr(G_F(\mathbf{U}, t) \leq 0) = \int_{\mathbf{u} \in \Omega_F^U(t)} \varphi_{n+1}(\mathbf{u})\, d\mathbf{u} \tag{12}$$

where $\varphi_{n+1}(\mathbf{u}) = \prod_{i=0}^{n} \varphi(u_i)$ is the $(n+1)$-variate standard normal PDF and $\varphi(\cdot)$ is the standard normal PDF.

3 System reliability updating of deteriorating structures

3.1 Modeling observations with likelihood functions

In the context of deteriorating structures, inspections and monitoring systems typically provide direct or indirect information on the uncertain deterioration model parameters **X**. This information is usually imperfect due to measurement uncertainties and random errors. Generally, parameters influencing the deterioration process, the deterioration state of the structure itself, and quantities indirectly related to the deterioration state of the structure can be observed. Examples of such observations are results from half-cell potential measurements that provide indirect information on corrosion initiation in reinforced concrete structures and measurements of fatigue cracks in welded steel structures.

Mathematically, an inspection or monitoring outcome i at time t is an event, which is denoted by $Z_i(t)$ in the following. The relationship between $Z_i(t)$ and the uncertain deterioration model parameters **X** is modeled through a likelihood function $L_i(\mathbf{x}, t)$, which is proportional to the conditional probability of observing $Z_i(t)$ when the uncertain parameters **X** take a value **x**:

$$L_i(\mathbf{x}, t) \propto \Pr(Z_i(t) | \mathbf{X} = \mathbf{x}) \tag{13}$$

Generally, two types of observations can be distinguished: observations providing equality information and observations providing inequality information (Madsen et al. 1986; Straub 2011a). Observations providing equality information are observations that can be described by an observation event such as $Z_i(t) = \{y_i(t) = q_i(\mathbf{X}, t) + E_i\}$, where $y_i(t)$ is a measurement of a continuous quantity predicted by the model $q_i(\mathbf{X}, t)$ and E_i is an additive measurement error with PDF $f_{E_i}(\epsilon_i)$. The following equality holds $Y_i(t) - q_i(\mathbf{X}, t) = E_i$, where $Y_i(t)$ is the uncertain measurement outcome. In this special but common case, the likelihood of observing $Y_i(t) = y_i(t)$ given $\mathbf{X} = \mathbf{x}$ is equal to the probability density of the random measurement error E_i taking the value $y_i(t) - q_i(\mathbf{x}, t)$. The corresponding likelihood function can be written as (Straub and Papaioannou 2015b):

$$L_i(\mathbf{x}, t) = f_{E_i}\big(y_i(t) - q_i(\mathbf{x}, t)\big) \tag{14}$$

In the general case, the likelihood function of an observation $Z_i(t)$ of the equality-type is defined as (Straub and Papaioannou 2015b):

$$L_i(\mathbf{x}.t) = f_{Y_i(t)|\mathbf{X}}(y_i(t)|\mathbf{x}) \tag{15}$$

where $f_{Y_i(t)|\mathbf{X}}(y_i(t)|\mathbf{x})$ is the conditional PDF of the uncertain measurement outcome $Y_i(t)$ given $\mathbf{X} = \mathbf{x}$, which is typically defined in terms of the PDF of the associated measurement error E_i. The likelihood function defined in Equation (15) includes the evaluation of the model predicting the measured quantity as in Equation (14).

Observations providing inequality information are observations such as "corrosion progress is larger than a limit" or "no fatigue crack detected". An observation $Z_i(t)$ of the inequality type is modeled through a function $q_i(\mathbf{X}, t)$ as follows (Madsen et al. 1986):

$$Z_i(t) = \{q_i(\mathbf{X}, t) \leq 0\} \tag{16}$$

A function $q_i(\mathbf{X}, t)$ of this type can be interpreted as a limit-state function. The corresponding likelihood function is written as (Straub and Papaioannou 2015b):

$$L_i(\mathbf{x}, t) = \Pr(Z_i(t)|\mathbf{X} = \mathbf{x}) = I(q_i(\mathbf{x}, t) \leq 0) \tag{17}$$

The value of such a likelihood function is either 0 or 1.

All observations obtained in the period $[0, t]$ are expressed by a combined event $Z_{0:t}$ as follows:

$$Z_{0:t} = \bigcap_{j=1}^{n_Z(t)} \left(\bigcap_{i \in S_j} Z_i(t_j) \right) \tag{18}$$

where $n_Z(t)$ is the number of times at which inspections or measurements are performed in the period $[0, t]$ and S_j is an index set containing the indices of all observations at time t_j. The likelihood function describing the relationship between $Z_{0:t}$ and the uncertain deterioration model parameters $\mathbf{X}$ is defined as:

$$L(\mathbf{x}, t) \propto \Pr(Z_{0:t}|\mathbf{X} = \mathbf{x}) \tag{19}$$

Under the common assumption that all individual observations are statistically independent given the deterioration model parameters $\mathbf{X} = \mathbf{x}$, $L(\mathbf{x}, t)$ is computed as:

$$L(\mathbf{x}, t) = \prod_{j=1}^{n_Z(t)} \left(\prod_{i \in S_j} L_i(\mathbf{x}, t_j) \right) \tag{20}$$

In the case of statistically dependent observations, the combined likelihood has to be formulated as a function of the joint distribution of all measurement errors. Straub and Papaioannou (2015a) provide further details on how to model observations with likelihood functions.

3.2 Posterior system failure probability

The goal here is to assess the effect of inspection and monitoring outcomes on the failure probability of deteriorating structural systems. In Bayesian analysis, this is achieved by computing the conditional probability of the failure event F_t given the observation event $Z_{0:t}$, which is defined as follows:

$$\Pr(F_t|Z_{0:t}) = \frac{\Pr(F_t \cap Z_{0:t})}{\Pr(Z_{0:t})} \tag{21}$$

We make the fundamental assumption that the system failure event F_t and the observation event $Z_{0:t}$ are conditionally independent given the deterioration model parameters $\mathbf{X} = \mathbf{x}$. The joint probability of the events F_t and $Z_{0:t}$ can therefore be written as:

$$\Pr(F_t \cap Z_{0:t}) = \int_{\boldsymbol{D}_\mathbf{X}} \Pr(F_t|\mathbf{X} = \mathbf{x}) \Pr(Z_{0:t}|\mathbf{X} = \mathbf{x}) \, f_\mathbf{X}(\mathbf{x}) \, d\mathbf{x} \tag{22}$$

The probability of the observation outcome event can also be expressed in the total-probability-form:

$$\Pr(Z_{0:t}) = \int_{\boldsymbol{D}_\mathbf{X}} \Pr(Z_{0:t}|\mathbf{X} = \mathbf{x}) \, f_\mathbf{X}(\mathbf{x}) \, d\mathbf{x} \tag{23}$$

Following Straub (2011a), the integrals in Equations (22) and (23) are transformed such that they can be solved using structural reliability methods. This method follows the same principles as presented in Section 2.3 for the computation of $\Pr(F_t)$.

For the purpose of transforming Equations (23), an auxiliary standard normal random variable P is again introduced. In addition, let c be a positive constant that ensures $0 \leq cL(\mathbf{x}, t) \leq 1$ for all $\mathbf{x}$. In this case, the following relationship holds:

$$cL(\mathbf{x}, t) = F_P\big(cL(\mathbf{x}, t)\big) = \Pr\big(P \leq cL(\mathbf{x}, t)\big) \tag{24}$$

The right hand side of Equation (24) corresponds to a component reliability problem with limit-state function:

$$g_{Z_e}(\mathbf{x}, p, t) = p - cL(\mathbf{x}, t) \tag{25}$$

The limit-state function $g_{Z_e}(\mathbf{x}, p, t)$ defines a domain $\Omega_{Z_e}(t)$ in the augmented outcome space of $\mathbf{X}$ and P as $\Omega_{Z_e}(t) = \big\{(\mathbf{x}, p) : g_{Z_e}(\mathbf{x}, p, t) \leq 0\big\}$. The quantity $\mathrm{c}L(\mathbf{x}, t)$ can be interpreted as the

290 conditional probability of P taking a value in $\Omega_{Z_e}(t)$ given $\mathbf{X} = \mathbf{x}$. It can thus be computed by
291 integrating $f_P(p)$ over the failure domain $\Omega_{Z_e}(t)$ when $\mathbf{X}$ take a value $\mathbf{x}$:

$$cL(\mathbf{x}, t) = \int_{p \in \Omega_{Z_e}(t)} f_P(p)\, dp = \int_0^1 I\big(g_{Z_e}(\mathbf{x}, p, t) \leq 0\big)\, f_P(p)\, dp \tag{26}$$

292 Consequently, the likelihood function $L(\mathbf{x}, t)$ can be written as:

$$L(\mathbf{x}, t) = \frac{1}{c} \int_0^1 I\big(g_{Z_e}(\mathbf{x}, p, t) \leq 0\big)\, f_P(p)\, dp \tag{27}$$

293 Let a denote the proportionality constant in the likelihood definition given in Equation (19). It
294 follows that:

$$\Pr(Z_{0:t} | \mathbf{X} = \mathbf{x}) = aL(\mathbf{x}, t) = \frac{a}{c} \int_0^1 I\big(g_{Z_e}(\mathbf{x}, p, t) \leq 0\big)\, f_P(p)\, dp \tag{28}$$

295 Inserting Equation (28) into Equation (23) gives:

$$\begin{aligned} \Pr(Z_{0:t}) &= \frac{a}{c} \int_{\boldsymbol{D}_\mathbf{X}} \left[\int_0^1 I\big(g_{Z_e}(\mathbf{x}, p, t) \leq 0\big)\, f_P(p)\, dp \right] f_\mathbf{X}(\mathbf{x})\, d\mathbf{x} \\ &= \frac{a}{c} \int_{(\mathbf{x}, p) \in \Omega_{Z_e}(t)} f_\mathbf{X}(\mathbf{x})\, f_P(p)\, d\mathbf{x}\, dp \end{aligned} \tag{29}$$

296 Similarly, it can be shown that the probability of the joint event $F_t \cap Z_{0:t}$ can be written as:

$$\Pr(F_t \cap Z_{0:t}) = \frac{a}{c} \int_{(\mathbf{x}, p) \in \Omega_{F \cap Z_e}(t)} f_\mathbf{X}(\mathbf{x})\, f_P(p)\, d\mathbf{x}\, dp \tag{30}$$

297 where the domain $\Omega_{F \cap Z_e}(t)$ is defined in the augmented outcome space of $\mathbf{X}$ and P in terms of the
298 limit-state function:

$$g_{F \cap Z_e}(\mathbf{x}, p, t) = p - p_F(\mathbf{x}, t) \cdot cL(\mathbf{x}, t) \tag{31}$$

299 as $\Omega_{F \cap Z_e}(t) = \big\{(\mathbf{x}, p) : g_{F \cap Z_e}(\mathbf{x}, p, t) \leq 0\big\}$.

300 Inserting Equation (29) and Equation (30) into Equation (21) gives:

$$\Pr(F_t | Z_{0:t}) = \frac{\int_{(\mathbf{x}; p) \in \Omega_{F \cap Z_e}(t)} f_\mathbf{X}(\mathbf{x}) f_P(p)\, d\mathbf{x}\, dp}{\int_{(\mathbf{x}; p) \in \Omega_{Z_e}(t)} f_\mathbf{X}(\mathbf{x}) f_P(p)\, d\mathbf{x}\, dp} = \frac{\Pr\big(g_{F \cap Z_e}(\mathbf{X}, P, t) \leq 0\big)}{\Pr\big(g_{Z_e}(\mathbf{X}, P, t) \leq 0\big)} \tag{32}$$

Note that the proportionality constant a vanishes. The numerator and the denominator in Equation (32) correspond to component reliability problems, which can be solved using structural reliability methods.

The solution given in Equation (32) can be interpreted as follows. The denominator in Equation (32) corresponds to the probability of an inequality observation event $Z_{e,0:t} = \{g_{Z_e}(\mathbf{X}, P, t) \leq 0\}$ and the numerator is equal to the probability of the joint event $F_t \cap Z_{e,0:t} = \{g_{F \cap Z_e}(\mathbf{X}, P, t) \leq 0\}$. In the context of Bayesian updating, the event $Z_{e,0:t}$ is equivalent to the original observation event $Z_{0:t}$ in the sense that:

$$\Pr(F_t | Z_{0:t}) = \Pr(F_t | Z_{e,0:t}) = \frac{\Pr(F_t \cap Z_{e,0:t})}{\Pr(Z_{e,0:t})} \tag{33}$$

For applying structural reliability methods, the component reliability problems defined in Equation (32) are also transformed to standard normal space following Section 2.3. The corresponding limit-state functions $G_{F \cap Z_e}$ and G_{Z_e} in **U**-space are:

$$G_{F \cap Z_e}(\mathbf{u}, t) = u_0 - \Phi^{-1}\left(p_F(\mathbf{T}^{-1}(u_1, \dots, u_n), t) \cdot cL(\mathbf{T}^{-1}(u_1, \dots, u_n), t)\right) \tag{34}$$

and

$$G_{Z_e}(\mathbf{u}, t) = u_0 - \Phi^{-1}\left(cL(\mathbf{T}^{-1}(u_1, \dots, u_n), t)\right) \tag{35}$$

These limit-state functions respectively describe the domains $\Omega^U_{F \cap Z_e}(t) = \{\mathbf{u} : G_{F \cap Z_e}(\mathbf{u}, t) \leq 0\}$ and $\Omega^U_{Z_e}(t) = \{\mathbf{u} : G_{Z_e}(\mathbf{u}, t) \leq 0\}$ in the transformed space. Consequently, the probabilities $\Pr(F_t \cap Z_{e,0:t})$ and $\Pr(Z_{e,0:t})$ can be computed as:

$$\Pr(F_t \cap Z_{e,0:t}) = \Pr(G_{F \cap Z_e}(\mathbf{U}, t) \leq 0) = \int_{\mathbf{u} \in \Omega^U_{F \cap Z_e}(t)} \varphi_{n+1}(\mathbf{u})\, d\mathbf{u} \tag{36}$$

and

$$\Pr(Z_{e,0:t}) = \Pr(G_{Z_e}(\mathbf{U}, t) \leq 0) = \int_{\mathbf{u} \in \Omega^U_{Z_e}(t)} \varphi_{n+1}(\mathbf{u})\, d\mathbf{u} \tag{37}$$

The computation of the integrals in Equations (36) and (37) requires the selection of the constant c. A discussion on how to select c is provided in (Betz et al. 2014b; Au et al. 2015; Straub and Papaioannou 2015b). In the general case, the optimal choice is $c = 1/\sup(L(\mathbf{x}, t))$ where $\sup(\cdot)$ is the supremum of the expression $(\cdot)$. In some cases, $\sup(L(\mathbf{x}, t))$ can be readily selected. For instance, in the special case of a single measurement with measurement error E, the supremum of the likelihood function is $\sup(L(\mathbf{x}, t)) = \max(f_E(\epsilon))$ where $f_E(\epsilon)$ is the PDF of E.

4 Computing system failure probabilities with subset simulation

Subset simulation, originally proposed by Au and Beck (2001), is an adaptive Monte Carlo method particularly suitable for evaluating the high-dimensional reliability problems defined in Equations (12), (36) and (37). The method is robust and computationally efficient, and it can be implemented relatively easily. The algorithm is here implemented following Papaioannou et al. (2015).

First, consider the computation of the prior system failure probability $\Pr(F_t) = \Pr(G_F(\mathbf{U}, t) \leq 0)$. The basic idea of subset simulation is to express the event F_t as an intersection of M intermediate events:

$$F_t = E_1 \cap E_2 \cap \ldots \cap E_M \tag{38}$$

The intermediate events are nested, i.e. $E_1 \supset E_2 \supset \cdots \supset E_M = F_t$. Consequently, the probability of the event F_t can be computed by a product of conditional probabilities:

$$\Pr(F_t) = \Pr(E_1 \cap E_2 \cap \ldots \cap E_M) = \prod_{i=1}^{M} \Pr(E_i | E_{i-1}) \tag{39}$$

In this formulation, the event E_0 is the certain event. The intermediate events are selected such that the conditional probabilities $\Pr(E_i|E_{i-1})$, $i = 1, \ldots, M$ are much larger than $\Pr(F_t)$. In this way, the original problem of evaluating the small probability of the rare event F_t reduces to computing a sequence of M larger conditional probabilities.

The intermediate events E_i, $i = 1, \ldots, M$ are defined as $E_i = \{G_F(\mathbf{U}, t) \leq b_i\}$ where $b_1 > b_2 > \cdots > b_M = 0$. The values of b_i are selected adaptively such that the conditional probabilities are equal to a chosen value p_0. For this purpose, N samples of $\mathbf{U}$ are simulated at each subset level i, conditional on the previous intermediate event E_{i-1}. For each generated sample, the limit-state function $G_F(\mathbf{u}, t)$ is evaluated and b_i is set equal to the p_0-percentile of the N resulting values of $G_F(\mathbf{u}, t)$. This procedure is repeated until the p_0-percentile becomes negative. At this stage, the failure event $E_M = F_t$ is reached, for which $b_M = 0$. The samples conditional on the event E_0 are obtained by crude Monte Carlo sampling. The samples conditional on the events $E_i, i = 1, \ldots, M-1$ are generated by simulating states of Markov chains starting from the samples conditional on E_{i-1}, for which $G_F(\mathbf{u}, t) \leq b_i$. This is achieved by application of Markov Chain Monte Carlo (MCMC) sampling. An estimator $\hat{P}_{SuS}$ of the prior system failure probability $\Pr(F_t)$ can now be written as:

$$\Pr(F_t) \approx \hat{P}_{SuS} = p_0^{M-1} \hat{P}_M \tag{40}$$

$\hat{P}_M$ is the estimate of the conditional probability $\Pr(E_M|E_{M-1})$, which is given by the ratio of the number of samples for which $G_F(\mathbf{u}, t) \leq 0$ over the number of samples N simulated conditional on E_{M-1}.

Note that the MCMC samples are generally not statistically independent. Their correlation has an effect on the efficiency and accuracy of subset simulation (see, for example, Au and Beck 2001; Schuëller and Pradlwarter 2007; Papaioannou et al. 2015). It is important to adopt an MCMC sampling algorithm that produces samples with low correlation such that the conditional probabilities $\Pr(E_i|E_{i-1})$ can be estimated with a minimum number of samples. We adopt the adaptive MCMC sampling algorithm of Papaioannou et al. (2015).

The value p_0 of the conditional probabilities and the number of simulated samples N at each subset level can be chosen freely. A value of $p_0 = 0.1$ is a suitable choice. N should be selected large enough to give accurate estimates of p_0. Note that the total number of required samples for estimating $\Pr(F_t)$ increases linearly with $-\log_{10}(\Pr(F_t))$ when using subset simulation instead of with $1/\Pr(F_t)$ when using crude Monte Carlo simulation (Au and Beck 2001).

The probabilities $\Pr(F_t \cap Z_{e,0:t}) = \Pr(G_{F\cap Z_e}(\mathbf{U},t) \leq 0)$ and $\Pr(Z_{e,0:t}) = \Pr(G_{Z_e}(\mathbf{U},t) \leq 0)$ are calculated accordingly. The posterior system failure probability $\Pr(F_t|Z_{0:t})$ is then computed using Equation (21). Alternatively, the conditional probability $\Pr(F_t|Z_{0:t}) = \Pr(F_t|Z_{e,0:t})$ can be estimated directly with a new subset simulation run following the estimation of $\Pr(Z_{e,0:t})$ (see also Schneider et al. 2013; Straub et al. 2016). For this purpose, a set of nested intermediate events $E_0 \supset E_1 \supset \cdots \supset E_M$ is defined where $E_0 = Z_{e,0:t}$, $E_i = \{G_{F\cap Z_e}(\mathbf{U},t) \leq b_i\}$, $i = 1,\dots,M$ and $b_1 > b_2 > \cdots > b_M = 0$. The conditional probability $\Pr(F_t|Z_{0:t})$ can now be expressed as:

$$\Pr(F_t|Z_{0:t}) = \Pr(E_1 \cap E_2 \cap \dots \cap E_M|E_0) = \prod_{i=1}^{M} \Pr(E_i|E_{i-1}) \tag{41}$$

The first threshold b_1 defining the intermediate event $E_1 = \{G_{F\cap Z_e}(\mathbf{U},t) \leq b_1\}$ is determined from the samples conditional on $E_0 = Z_{e,0:t}$, which are obtained as a by-product of estimating $\Pr(Z_{e,0:t})$ with subset simulation. The remaining thresholds b_i, $i = 2,\dots,M-1$ are determined following the original subset simulation procedure. When applying this approach, the estimator $\hat{P}_{SuS}$ defined in Equation (40) provides an estimate of the conditional probability $\Pr(F_t|Z_{0:t})$.

5 Application a: Zayas frame subjected to fatigue deterioration

We consider the two-dimensional welded steel frame shown in Figure 1, which is known as Zayas frame (Zayas et al. 1980). The critical load scenario is an environmental load L. In addition, the frame is subjected to fatigue loads throughout its service life of $T = 50$ years. The effect of inspections on the fatigue reliability of the elements and on the reliability of the complete structural system is studied.

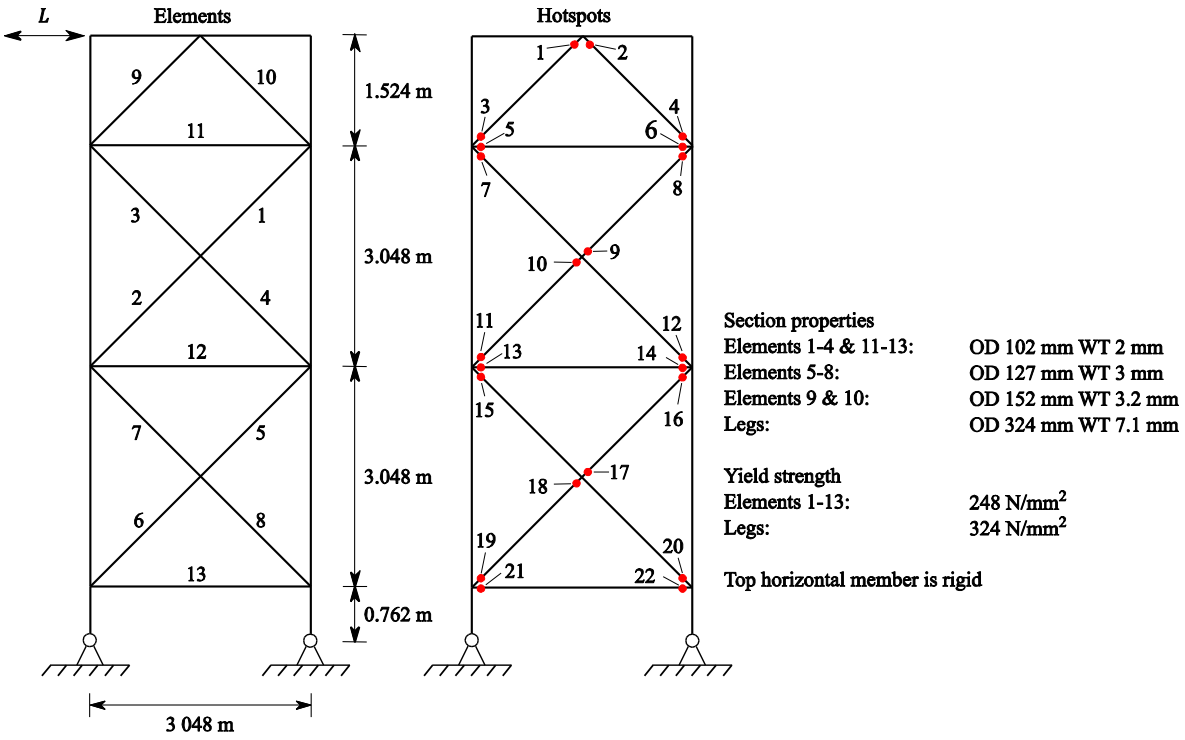

Figure 1. Zayas frame (Zayas et al. 1980). OD is the outer diameter and WT is the wall thickness of the tubular steel members.

5.1 System model

The Zayas frame consists of tubular steel elements with welded connections. The state of fatigue deterioration of any element i depends on the condition of the associated welded connections. Fatigue cracks usually develop at locations with local stress concentrations; welded connections are especially vulnerable due to material inhomogeneities, imperfections, high stress concentrations and residual stresses (Fricke 2003). Locations where fatigue cracks may develop are called hotspots. A welded connection may contain multiple hotspots.

Fatigue crack growth reduces the capacity of welded connections. In the current example, we assume that fatigue deterioration occurs at the welds connecting the braces with the legs and with the upper horizontal element as well as at the welds at the intersection of the X-braces. Furthermore, we assume that each deteriorating welded connection contains only one critical hotspot. Thus, there are $n_E = 13$ deteriorating elements and $n_H = 22$ hotspots as indicated in Figure 1.

The approach of Straub and Der Kiureghian (2011) is adopted to determine the reliability of the welded steel structure subjected to fatigue. At system level, no gradual degradation of weld capacities is considered. At a given time t, a welded connection has either its full capacity or it has completely lost its capacity because of fatigue crack growth. In the current example, we assume that a welded connection loses its capacity if a fatigue crack at any of the associated hotspots grows beyond a critical size (e.g. Madsen 1997). Thus, the deterioration state of any hotspot j at time t

is modeled by a binary random variable $D_{H,j,t}$, where $\{D_{H,j,t} = 1\}$ is the hotspot fatigue damage event and $\{D_{H,j,t} = 0\}$ is the compliment. The event of fatigue damage of hotspot j at time t is defined by a limit-state function $g_{H,j}(\mathbf{x}, t)$ as $\{D_{H,j,t} = 1\} = \{g_{H,j}(\mathbf{X}, t) \leq 0\}$ where $\mathbf{X}$ denotes the vector of all uncertain parameters that describe fatigue deterioration of all hotspots considered in the system reliability analysis. $g_{H,j}(\mathbf{x}, t)$ is written as:

$$g_{H,j}(\mathbf{x}, t) = a_{c,j} - a_j(\mathbf{x}, t) \tag{42}$$

where $a_{c,j}$ is the critical crack size and $a_j(\mathbf{x}, t)$ is the fatigue crack size at hotspot j at time t. $a_j(\mathbf{x}, t)$ is computed by means of a probabilistic fatigue crack growth model presented in Section 5.2. $a_{c,j}$ may be defined such that failure modes such as plastic collapse or unstable crack growth are approximately accounted for.

A structural element loses its capacity if any of the associated welded connections loses its capacity. It follows that an element fails as soon as any of the associated hotspots fails due to fatigue deterioration; this corresponds to a series system. The deterioration state of any element i at time t is, therefore, also modeled by a binary random variable $D_{i,t}$ where $\{D_{i,t} = 1\}$ is the event of element fatigue failure and $\{D_{i,t} = 0\}$ is the compliment. From system reliability theory it follows that the event of fatigue failure of element i can be written as:

$$\{D_{i,t} = 1\} = \bigcup_{j \in C_i} \{D_{H,j,t} = 1\} \tag{43}$$

where C_i is an index set containing the indices of all hotspots associated with element i. The event of fatigue failure of element i can also be expressed by a limit-state function $g_i(\mathbf{x}, t)$ such that $\{D_{i,t} = 1\} = \{g_i(\mathbf{X}, t) \leq 0\}$. $g_i(\mathbf{x}, t)$ is defined as a combination of the individual hotspot limit-state functions $g_{H,j}(\mathbf{x}, t)$, $\forall j \in C_i$ as:

$$g_i(\mathbf{x}, t) = \min_{j \in C_i} g_{H,j}(\mathbf{x}, t) \tag{44}$$

The function h_i defining the relationship between the fatigue model parameters $\mathbf{X}$ and the element deterioration state $D_{i,t}$ can now be written as:

$$D_{i,t} = h_i(\mathbf{X}, t) = I(g_i(\mathbf{X}, t) \leq 0) \tag{45}$$

Using Equation (2), the system deterioration state $\mathbf{D}_t = (D_{1,t}, \dots, D_{n_E,t})$ of the Zayas frame can subsequently be calculated as a function of the uncertain fatigue model parameters $\mathbf{X}$. In the current example, $\mathbf{D}_t$ is a binary random vector with 2^{n_E} states.

The Zayas frame is subjected to a time-variant horizontal load whose annual maximum L has the Gumbel distribution with a coefficient of variation (c.o.v.) $\delta_L = 0.35$. The CDF of L is denoted by

$F_L(l)$. Material and geometry properties are modeled as deterministic parameters as listed in Figure 1. This simplification is reasonable since the uncertainties associated with these quantities are small compared to the uncertainties associated with the system deterioration state and the load L. It is thus possible to determine a deterministic ultimate horizontal capacity $r(\mathbf{d}_t)$ of the damaged Zayas frame for any realization of the system deterioration state $\mathbf{D}_t = \mathbf{d}_t$. Consequently, the conditional probability of system failure $p_F(\mathbf{x}, t)$ of the Zayas frame corresponds to the probability that the annual maximum load L exceeds the ultimate capacity $r(\mathbf{d}_t)$:

$$\Pr(F_t|\mathbf{D}_t = \mathbf{d}_t) = \Pr(r(\mathbf{d}_t) \leq L) = 1 - F_L\big(r(\mathbf{d}_t)\big) \tag{46}$$

The mean of L is selected such that the undamaged Zayas frame has an annual probability of system failure $\Pr(F_t|\mathbf{D}_t = \mathbf{0}) = 1.3 \times 10^{-6}$, leading to $\mu_L = 62$ kN.

In the current example, $r(\mathbf{d}_t)$ is computed by performing pushover analysis of the structure with all elements damaged according to $\mathbf{D}_t = \mathbf{d}_t$, i.e. all elements with fatigue failure are removed from the model used in the pushover analysis. Through such analyses the ultimate capacity of framed steel structures can be quantified. Non-linear effects associated with non-linear material behavior, imperfections, large displacements and deformations (large strains) are modelled explicitly. The analysis captures load redistribution within the structural system resulting from local stiffness changes. It simulates the collapse process of the structural system including initial yielding, formation of plastic hinges, member buckling as well as formation of a global system collapse mechanism (see e.g. Ultiguide 1999; Skallerud and Amdahl 2002).

In the current study, $2^{13} = 8192$ pushover analyses are carried out using USFOS (2014) to pre-calculate the maximum resistance $r(\mathbf{d}_t)$ for all possible realizations of the system deterioration state $\mathbf{D}_t$. The corresponding conditional system failure probabilities $\Pr(F_t|\mathbf{D}_t = \mathbf{d}_t)$ are computed according to Equation (46). These failure probabilities have a reference period $\Delta t = 1$ year but are independent of time. In the subsequent reliability analysis of the deteriorating Zayas frame, the computation of $p_F(\mathbf{x}, t)$ is thus reduced to a lookup operation in which a realization of the fatigue model parameters $\mathbf{x}$ is matched to a pre-calculated conditional system failure probability $\Pr(F_t|\mathbf{D}_t = \mathbf{d}_t)$ at time t by means of Equation (3), i.e. $\mathbf{d}_t = \mathbf{h}(\mathbf{x}, t)$.

The influence of individual element failure on the reliability of the Zayas frame depends on the structural importance of the failed element. Following Straub and Der Kiureghian (2011), the structural importance of an element i is quantified in terms of the single-element importance measure SEI_i, which is defined as the difference in the failure probability of the undamaged system and the failure probability of the system in which only element i has failed due to fatigue deterioration.

$$\mathrm{SEI}_i = \Pr\big(F_t|D_{1,t} = 0, \dots, D_{i-1,t} = 0, D_{i,t} = 1, D_{i+1,t} = 0, \dots, D_{n_E,t} = 0\big) - \Pr(F_t|\mathbf{D}_t = \mathbf{0}) \tag{47}$$

Table 1 summarizes the single-element importance measures for all deteriorating elements considered in the system reliability analysis of the Zayas frame.

Table 1. Single-element importance (SEI) measure and structural importance category of all deteriorating elements of the Zayas frame.

Element i	SEI_i	Structural importance category
1, 3	1.14×10^{-5}	Medium
2, 4	1.06×10^{-5}	Medium
5, 7	1.99×10^{-3}	High
6, 8	2.00×10^{-3}	High
9, 10	7.25×10^{-7}	Low
11	8.26×10^{-8}	Low
12	6.31×10^{-7}	Low
13	2.27×10^{-7}	Low

The lower X-braces (elements 5 to 8) are the most important elements followed by the X-braces at the level above (elements 1 to 4). The top braces (elements 9 and 10) and the horizontal braces (elements 11 to 13) are the least important elements.

5.2 Fatigue model

In the current example, we adopt the widely used Paris' law (Paris and Erdogan 1963) to describe fatigue crack growth at a given hotspot. For illustration purposes, we consider a through-thickness fatigue crack in an infinite plate subjected to fluctuating stresses in the plane of the plate and orthogonal to the crack. In this case, the fatigue crack is fully characterized by its length $2a$ and Paris' law is written as:

$$\frac{da(n)}{dn} = C\left(\Delta S(n)\sqrt{\pi a(n)}\right)^m \tag{48}$$

$da(n)/dn$ is the crack growth rate, n is the number of applied fatigue stress cycles, C and m are empirical material parameters and $\Delta S(n)$ is the varying far-field fatigue stress range. The quantity $\Delta K = \Delta S(n)\sqrt{\pi a(n)}$ is the stress intensity factor (SIF) range. This model can be extended to account for more complex fatigue crack and hotspot geometries as well as more complex fatigue stress distributions (Straub 2004). If desired, the model can be replaced altogether with a more advanced crack growth model (e.g. Altamura and Straub 2014). This will not affect the method as described in the remainder of the paper.

Fatigue loads are generally random and the load sequence $\Delta S(n)$ is ideally modeled by a stochastic process (Altamura and Straub 2014). Under the condition that the fatigue stress process is

stationary, ergodic and sufficiently mixing, a simplified approach can be adopted where the crack growth rate $da(n)/dn$ given by Equations (48) is approximated by its expected value with respect to ΔS:

$$\frac{da(n)}{dn} \approx E_{\Delta S}\left[C\left(\Delta S(n)\sqrt{\pi a(n)}\right)^m\right] = C\left(\sqrt{\pi a(n)}\right)^m E_{\Delta S}[\Delta S(n)^m] \tag{49}$$

The fatigue stress process is described by its stationary distribution $f_{\Delta S}(\Delta S)$ and an annual stress cycle rate ν (e.g. Madsen et al. 1986). The quantity $\Delta S_e = (E_{\Delta S}[\Delta S(n)^m])^{1/m}$ is interpreted as an equivalent stress range. In the current example, we assume that the stationary distribution of the fatigue stress ranges $f_{\Delta S}(\Delta S)$ can be modeled by a Weibull distribution. The equivalent stress range is hence given by:

$$\Delta S_e = (E_{\Delta S}[\Delta S(n)^m])^{1/m} = k\Gamma\left(1+\frac{m}{\lambda}\right)^{1/m} \tag{50}$$

$\Gamma(\cdot)$ denotes the Gamma function and k and λ are the Weibull scale and shape parameters. k is modeled as a lognormal random variable to model statistical uncertainties in the calculation of ΔS_e; λ is assumed to be deterministic.

The parameters C and m of Paris' law are modeled as time-invariant random variables to capture uncertainties due to the variability of the material properties and material inhomogeneities. Proper attention has to be paid to modeling the correlation among C and m. They are empirical parameters generally derived from the same experiments and are therefore strongly correlated. To model the dependence among the Paris' law parameters, the linear relationship between $\ln C$ and m given in (Gurney 1978) is adopted:

$$\ln C = -15.84 - 3.34m \tag{51}$$

Equation (51) is valid if stresses are given in N/mm^2 and the crack growth rate is given in m/cycle. In the following, C is modeled as a lognormally distributed random variable. m is thus normal distributed due to the linear relationship between $\ln C$ and m.

To capture uncertainties in the fabrication quality, the initial crack size a_0 is modeled as a random variable with exponential distribution. Uncertainties in the calculation of the hotspot stress and in the calculation of the SIF range are captured by introducing lognormal random bias factors $B_{\Delta S}$ and B_{SIF}, which are multiplied with the calculated equivalent stress range ΔS_e. The one-dimensional crack growth model given in Equation (48) is rewritten as:

$$\frac{da(n)}{dn} = C\left(B_{SIF}B_{\Delta S}\Delta S_e\sqrt{\pi a(n)}\right)^m \tag{52}$$

With $a_j(n=0)=a_{0,j}$ as initial condition, the differential equation given by Equation (52) is solved for the fatigue crack size a_j at hotspot j as a function of time t (Madsen et al. 1986):

$$a_j(\mathbf{X},t)=\begin{cases}\left[\left(1-\frac{m_j}{2}\right)C_j B_{SIF,j}^{m_j} B_{\Delta S,j}^{m_j} \Delta S_{e,j}^{m_j} \pi^{\frac{m_j}{2}} \nu_j t + a_{0,j}^{\left(1-\frac{m_j}{2}\right)}\right]^{\left(1-\frac{m_j}{2}\right)^{-1}}, & m_j \neq 2 \\ a_{0,j}\exp\left(C_j B_{SIF,j}^2 B_{\Delta S,j}^2 \Delta S_{e,j}^2 \pi \nu_j t\right), & m_j = 2\end{cases} \quad (53)$$

where t is the time in years, ν_j is the annual stress cycle rate and $\nu_j t$ is the total number of stress cycles in the period $[0,t]$. $\Delta S_{e,j}$ is computed as a function of k_j, λ_j and m_j according to Equation (50). The vector of all uncertain parameters describing fatigue deterioration of all hotspots considered in the system reliability analysis is defined as:

$$\mathbf{X}=\left(C_1, m_1, a_{0,1}, B_{SIF,1}, B_{\Delta S,1}, k_1, \ldots, C_{n_H}, m_{n_H}, a_{0,n_H}, B_{SIF,n_H}, B_{\Delta S,n_H}, k_{n_H}\right) \quad (54)$$

The same probabilistic models are applied to describe the crack growth model parameters for all hotspots $j=1,\ldots,n_H$. They are summarized in Table 2.

Table 2. Probabilistic models of the fatigue crack growth parameters for all hotspots $j=1,\ldots,n_H$.

Parameter	Dimension	Distribution	Mean	Standard deviation
$\ln k_j$	corresponding to N/mm^2	normal	2.0	0.275
λ_j	-	deterministic	0.8	-
ν_j	yr^{-1}	deterministic	$5\cdot10^6$	-
$a_{0,j}$	mm	exponential	0.11	0.11
$a_{c,j}$	mm	deterministic	20	-
$\ln C_j$	corresponding to N and mm	normal	-29.97	0.514
m_j	-	normal	calculated from $\ln C_j = -15.84 - 3.34 m_j$	
$B_{\Delta S,j}$	-	lognormal	1.0	0.1
$B_{SIF,j}$	-	lognormal	1.0	0.1

The mean and standard deviation of the equivalent stress range $\Delta S_{e,j}$ are a function of the distributions of $\ln k_j$ and $\ln C_j$ through Equations (50) and (51). They are $\mu_{\Delta S_{e,j}} = 20.1$ N/mm^2 and $\sigma_{\Delta S_{e,j}} = 5.65$ N/mm^2.

Statistical dependence among hotspot fatigue behavior is modeled through correlation coefficients among the fatigue model parameters. In the current example, the fatigue model parameters $a_{0,j}$, C_j, k_j, $B_{\Delta S,j}$ and $B_{SIF,j}$ are equi-correlated among all hotspots $j=1,\ldots,n_H$ with correlation coefficients ρ_{a_0}, $\rho_{\ln C}$, $\rho_{\ln k}$, $\rho_{B_{\Delta S}}$ and $\rho_{B_{SIF}}$. The correlation coefficient ρ_{a_0} represents the statistical dependence due to common fabrication quality; $\rho_{\ln C}$ reflects the statistical dependence

due to common material characteristics; $\rho_{\ln k}$ models the statistical dependence due to common loading characteristics; and $\rho_{B_{\Delta S}}$ and $\rho_{B_{SIF}}$ describe statistical dependence due to common uncertainties in the calculation of hotspot fatigue stress ranges and SIF ranges. The joint distribution of all fatigue model parameters in **X** is subsequently modeled through a Gaussian copula (Nataf) model (Liu and Der Kiureghian 1986).

To study the influence of different levels of statistical dependence among hotspot fatigue behavior, three different dependence cases are considered (low, medium, high), which are defined in terms of the correlation coefficients ρ_{a_0}, $\rho_{\ln C}$, $\rho_{\ln k}$, $\rho_{B_{\Delta S}}$ and $\rho_{B_{SIF}}$ as listed in Table 3.

Table 3. Correlation coefficients among the fatigue crack growth parameters.

	low dependence	medium dependence	high dependence
ρ_{a_0}	0.2	0.5	0.8
$\rho_{\ln C}$	0.2	0.5	0.8
ρ_{lnk}	0.2	0.5	0.8
$\rho_{B_{\Delta S}}$	0.2	0.5	0.8
$\rho_{B_{SIF}}$	0.2	0.5	0.8

5.3 Inspection model

In the context of fatigue deterioration, relevant inspection outcomes are (a) no detection, (b) detection but no measurement, and (c) detection and measurement of a fatigue crack. These inspection outcomes are directly related to the crack size $a_j(\mathbf{X}, t)$ predicted for a given hotspot j at inspection time t. In the current study, we consider inspection outcomes of the type (a) and (b). The ability of an inspection method to detect a fatigue crack with a certain size $A = a$ is commonly described by a probability of detection curve $\pi(a)$, which is defined as:

$$\pi(a) = \Pr(\text{detection of a fatigue crack} | A = a) \tag{55}$$

Such a probability of detection curve describes the performance of the applied inspection method; it accounts for uncertain factors such as measurement errors, inspector performance and environmental conditions (Straub 2004). In the current case study, an exponential probability of detection curve is applied:

$$\pi(a) = 1 - \exp(-a/\lambda_D) \tag{56}$$

with $\lambda_D = 1.95$ mm. This probability of detection model is representative of magnetic particle inspection (Moan et al. 2000).

The likelihood function describing the inspection outcome $Z_i(t) = \{$fatigue crack detected at hotpot j at time $t\}$ is thus equal to the probability of detection:

$$L_i(\mathbf{x},t) = \pi\left(a_j(\mathbf{x},t)\right) \tag{57}$$

The likelihood function of the complementary inspection outcome $Z_i(t) = \{$no fatigue crack detected at hotpot j at time $t\}$ is:

$$L_i(\mathbf{x},t) = 1 - \pi\left(a_j(\mathbf{x},t)\right) \tag{58}$$

Under the common assumption that individual inspection outcomes are statistically independent given the crack sizes $a_j(\mathbf{x},t), j = 1,\dots,n_H$, the combined likelihood function $L(\mathbf{x},t)$ of all inspection outcomes $Z_{0:t}$ in the time period $[0,t]$ is given by Equation (20). If individual inspections are not statistically independent due to, for example, common influencing factors such as environmental conditions and inspector characteristics, the combined likelihood has to be formulated such that this aspect is captured. Approaches to modeling dependence among inspection outcomes are, for example, presented in (Straub and Faber 2003)(Maljaars and Vrouwenvelder 2014).

Since detection/no-detection events provide inequality information, the constant c that ensures $0 \leq cL(\mathbf{x},t) \leq 1$ for all $\mathbf{x}$ can be chosen as $c = 1$ (see also Section 3.1).

5.4 Prior system reliability analysis

The prior annual system failure probability $\Pr(F_t)$ of the Zayas frame is computed for each degree of dependence among hotspot fatigue behavior according to Equation (12). The results are shown in Figure 2. The problem is solved using subset simulation as described in Section 4 with conditional probabilities $p_0 = 0.1$ and $N = 1000$ samples per subset level. The statistics of the system failure probability are determined from 500 independent simulation runs. This approach is applied in all subsequent analyses presented in this paper.

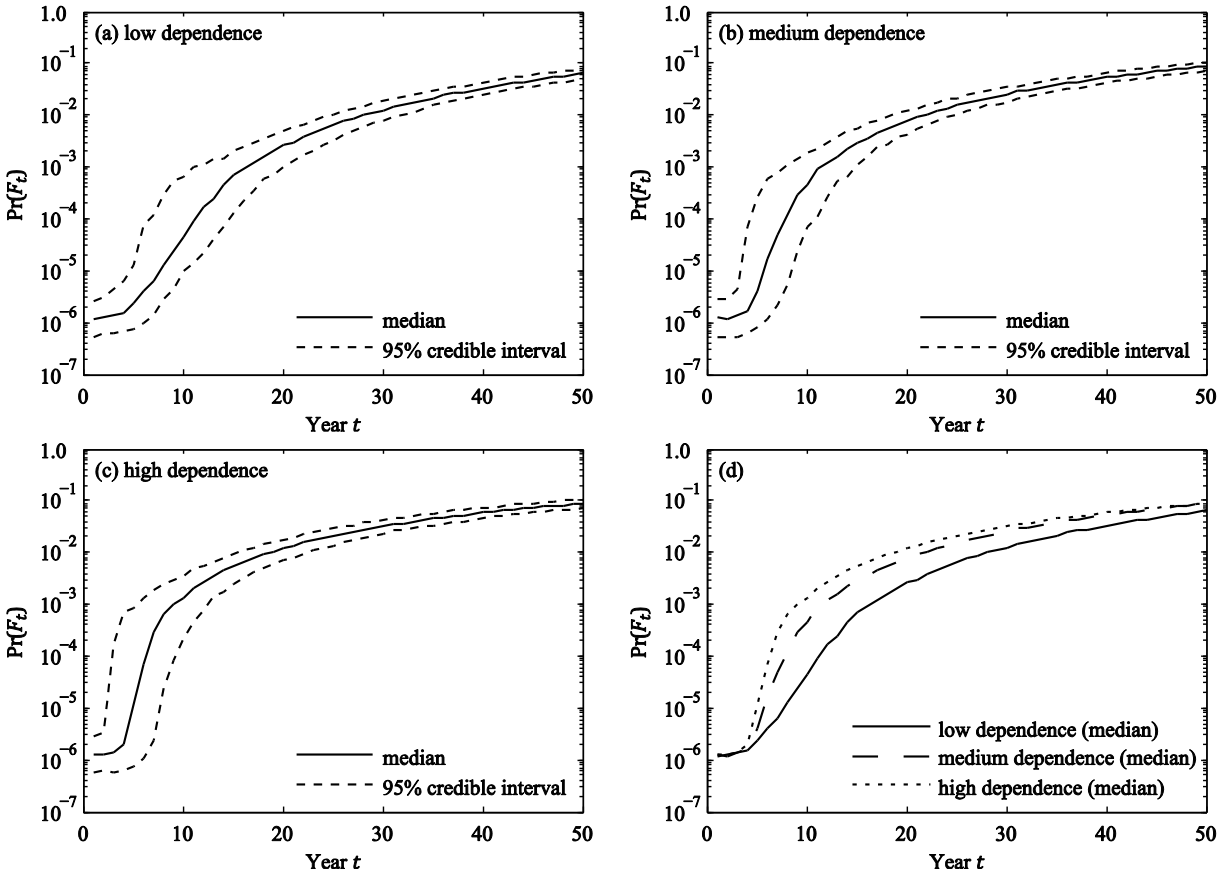

Figure 2. Median and 95% credible interval of the prior annual system failure probability $\Pr(F_t)$ of the Zayas frame as a function of different degrees of dependence among hotspot fatigue behavior. Computations are performed with subset simulation as summarized in Section 4 with conditional probabilities $p_0 = 0.1$ and $N = 1000$ samples per subset level. (d) compares the respective medians of the prior annual system failure probability.

As expected, the annual system failure probability $\Pr(F_t)$ increases with time t, due to fatigue deterioration. Furthermore, Figure 2(d) indicates that a higher dependence among hotspot fatigue behavior leads to a larger system failure probability due to an increase in the probability of joint occurrence of several element fatigue failures. This result is expected for a redundant structural system (Straub and Der Kiureghian 2011).

The width of the 95% credible interval indicates the accuracy of the employed subset simulation. The interval has 0.95 probability of containing the true value of the system failure probability (within the confines of the model). From Figure 2(a) to (c) it can be seen that the accuracy of the computation varies with time t since the number of samples per subset level used in the simulation is the same for all years. Results are less accurate for low values of t, because of the associated smaller system failure probability. Note, however, that the variability of the simulated failure probabilities at the beginning of the structure's service life ($t < 5$yr) is small. In this period, the probability of fatigue failures is very small, and they have little effect on the system failure probability (the failure probability of the undamaged Zayas frame is $\Pr(F_t|\mathbf{D}_t = \mathbf{0}) = 1.3 \cdot 10^{-6}$).

5.5 Posterior system reliability analysis

In this section, different inspection scenarios in terms of inspection times, coverage and outcomes are considered to study their effect on the reliability of the Zayas frame. Firstly, hotspots $\{5, 6, 13, 14, 21, 22\}$ are inspected at time $t = 10$ years. These hotspots are associated with the least important braces of the Zayas frame (see Figure 1 and Table 1). No fatigue cracks are detected during the inspection. The posterior annual system failure probability $\Pr(F_t|Z_{0:t})$, $t = 1, \ldots, 50$ are computed for each degree of dependence among hotspot fatigue behavior with subset simulation as described in Section 4 with conditional probabilities $p_0 = 0.1$ and $N = 1000$ samples per subset level. The results are shown in Figure 3.

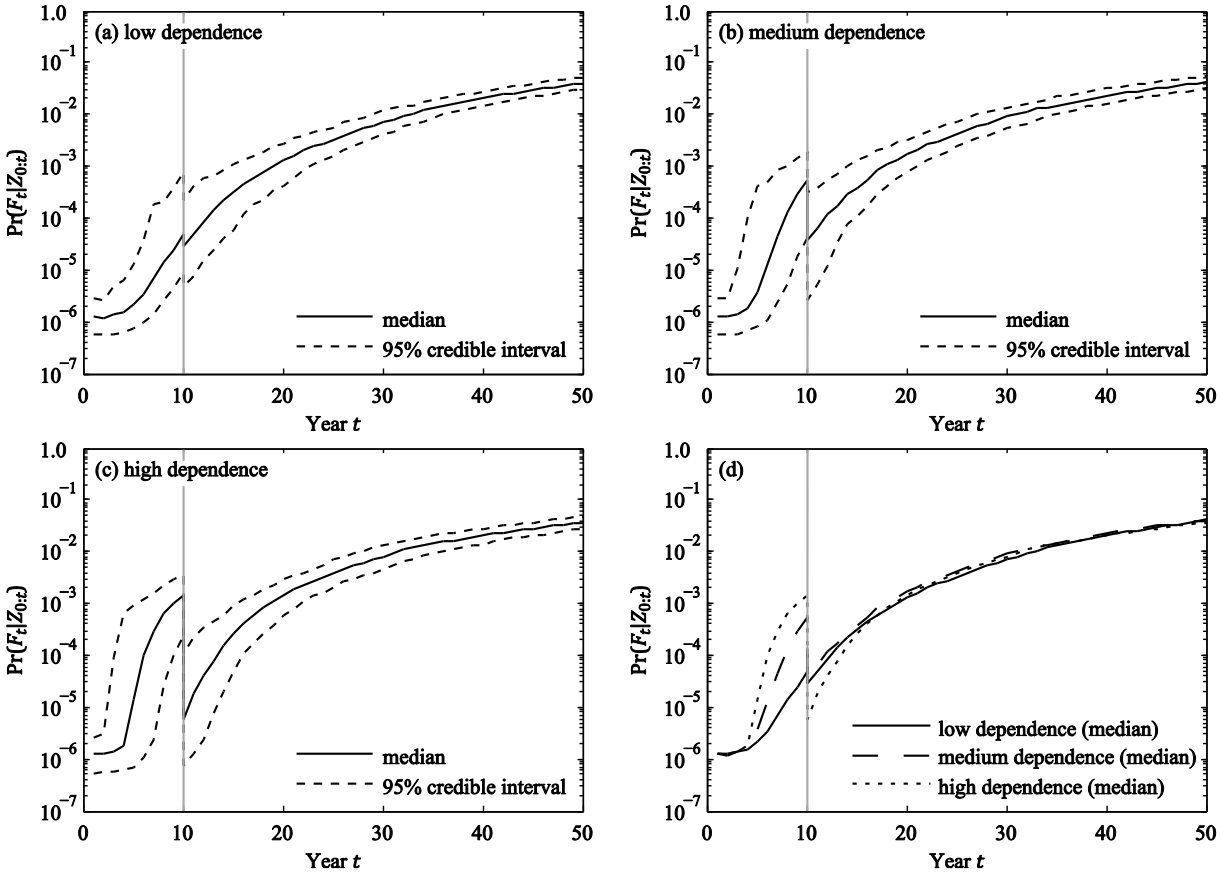

Figure 3. Median and 95% credible interval of the posterior annual system failure probability $\Pr(F_t|Z_{0:t})$ of the Zayas frame as a function of different degrees of dependence among hotspot fatigue behavior. Hotspots $\{5, 6, 13, 14, 21, 22\}$ are inspected at time $t = 10$ years. No fatigue cracks are detected. Computations are performed with subset simulation as summarized in Section 4 with conditional probabilities $p_0 = 0.1$ and $N = 1000$ samples per subset level. (d) compares the respective medians of the posterior annual system failure probability.

When considering the posterior medians of the estimated posterior system failure probabilities shown in Figure 3 (a) to (c), it can be seen that the system failure probability reduces after the inspection due to the positive inspection result. The effect increases with increasing degree of dependence among hotspot deterioration behavior.

607 Table 4 lists the probabilities $\Pr(Z_{e,0:t})$ and $\Pr(F_t|Z_{0:t})$ computed at time $t = 10$ years. The subset
608 simulation (SuS) results are presented together with those from additional Monte Carlo simulations
609 (MCS). The number of model evaluations is also provided for each simulation of $\Pr(F_t|Z_{0:t})$ to
610 indicate the computational efforts, since the accuracy can always be improved by increasing the
611 number of samples. The results in Table 4 show that the probability of the inspection outcome is
612 large. This is because the initial defects at each hotspot considered in the current case study are
613 small, and hence the fatigue cracks are unlikely to grow to a detectable size within the first 10
614 years of the structure's service life.

615 Table 4 Probability of the inspection outcome $\Pr(Z_{e,0:t})$ and the posterior system failure probability
616 $\Pr(F_t|Z_{0:t})$ at time $t = 10$ years. Subset simulation (SuS) is performed as summarized in Section 4 with
617 conditional probabilities $p_0 = 0.1$ and $N = 1000$ samples per subset level. Results in square brackets
618 represent the 95% credible interval. MCS is performed with 10^7 samples. Results are shown as 95%
619 confidence interval. The total number of model runs are provided for the computation of $\Pr(Z_{e,0:t})$ and
620 $\Pr(F_t|Z_{0:t})$.

Case	Method	$\Pr(Z_{e,0:t})$	$\Pr(F_t\|Z_{0:t})$	# model runs
Low dependence	SuS	$[0.642; 0.7]$	$[0.0467; 2.3] \cdot 10^{-4}$	$5.9 \cdot 10^3$
	MCS	$[0.671; 0.6716]$	$[7.08; 8.49] \cdot 10^{-5}$	10^7
Medium dependence	SuS	$[0.659; 0.717]$	$[0.0267; 3.11] \cdot 10^{-4}$	$5.9 \cdot 10^3$
	MCS	$[0.6875; 0.688]$	$[0.864; 1.01] \cdot 10^{-4}$	10^7
High dependence	SuS	$[0.673; 0.734]$	$[0.00758; 1.08] \cdot 10^{-4}$	$6.8 \cdot 10^3$
	MCS	$[0.7042; 0.7048]$	$[2.94; 3.79] \cdot 10^{-5}$	10^7

621

622 In the second example, hotspots $\{15,16,17,18,19,20\}$ are inspected at time $t = 10$ years. These
623 hotspots are associated with the most important structural members of the Zayas frame (see Figure
624 1 and Table 1). We assume again that each inspection results in a no-detection event. The posterior
625 annual system failure probability $\Pr(F_t|Z_{0:t})$ is shown for all three dependence cases in Figure 4.
626 In contrast to the first scenario, an inspection of the most important structural elements has a
627 significant effect on the system reliability regardless of the degree of dependence among element
628 deterioration.

629

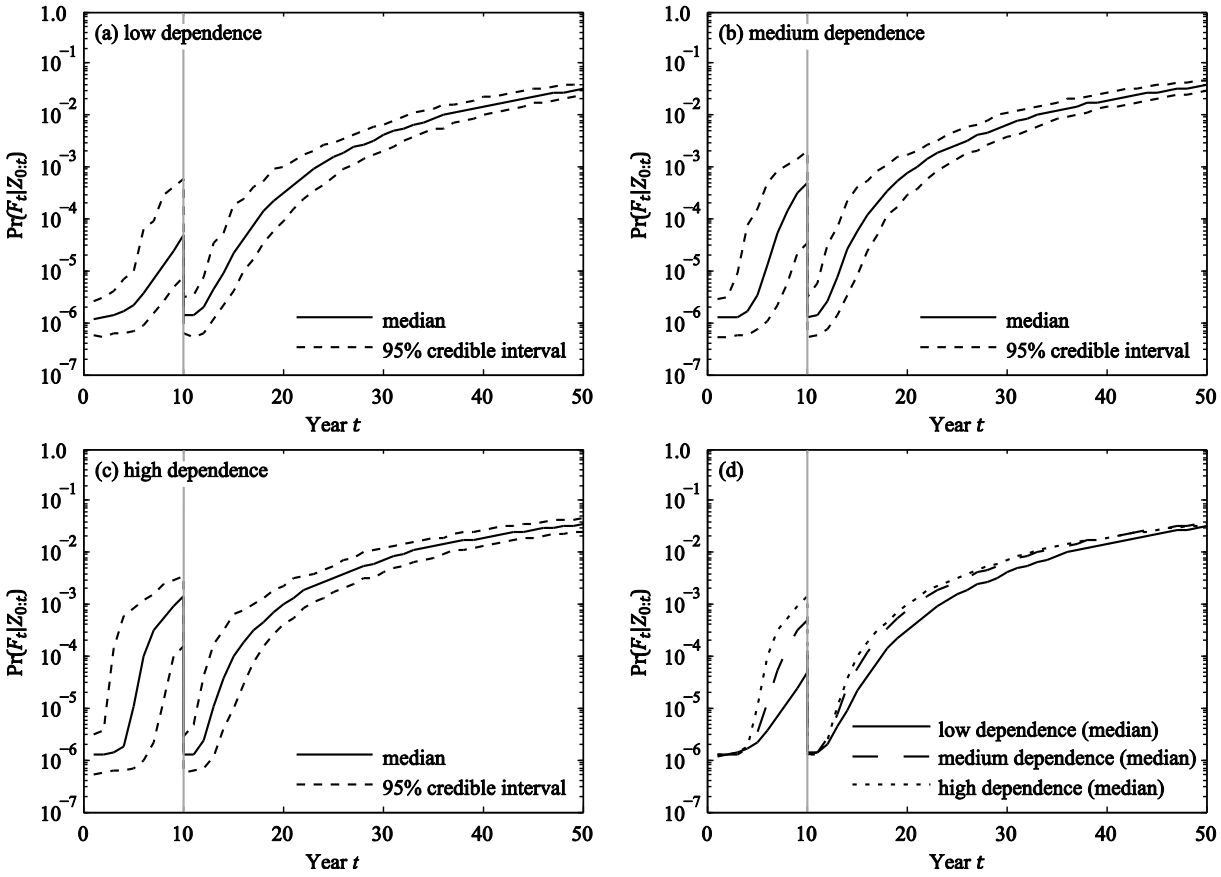

Figure 4. Median and 95% credible interval of the posterior annual system failure probability $\Pr(F_t|Z_{0:t})$ of the Zayas frame as a function of different degrees of dependence among hotspot fatigue behavior. Hotspots {15,16,17,18,19,20} are inspected at time $t = 10$ years. No fatigue cracks are detected. Computations are performed with subset simulation as summarized in Section 4 with conditional probabilities $p_0 = 0.1$ and $N = 1000$ samples per subset level. (d) compares the respective medians of the posterior annual system failure probability.

The probability of the inspection outcome $\Pr(Z_{e,0:t})$ and the posterior system failure probability $\Pr(F_t|Z_{0:t})$ at year 10 are summarized in Table 5 for each dependence case. The computed probabilities $\Pr(Z_{e,0:t})$ are the same as in the first scenario (see Table 4) because the applied probabilistic models of the crack growth parameters are identical for all hotspots (see Table 2). Comparing the bounds of the SuS and MCS results for $\Pr(F_t|Z_{0:t})$, it is seen that their accuracy is similar even though the number of samples in the SuS is only $N = 1000$ samples per subset level.

642 Table 5. Probability of the inspection outcome $\Pr(Z_{e,0:t})$ and the posterior system failure probability
643 $\Pr(F_t|Z_{0:t})$ at time $t = 10$ years. Subset simulation is performed as summarized in Section 4 with
644 conditional probabilities $p_0 = 0.1$ and $N = 1000$ samples per subset level. Results represent the 95%
645 credible interval. MCS is performed with 10^7 samples. Results represent the 95% confidence interval.

Case	Method	$\Pr(Z_{e,0:t})$	$\Pr(F_t\|Z_{0:t})$	# model runs
Low dependence	SuS	$[0.642; 0.701]$	$[0.635; 3.15] \cdot 10^{-6}$	$6.8 \cdot 10^3$
	MCS	$[0.671; 0.6716]$	$[1.22; 3.54] \cdot 10^{-6}$	10^7
Medium dependence	SuS	$[0.656; 0.715]$	$[0.543; 3.12] \cdot 10^{-6}$	$6.8 \cdot 10^3$
	MCS	$[0.6876; 0.6882]$	$[1.89; 4.53] \cdot 10^{-6}$	10^7
High dependence	SuS	$[0.673; 0.73]$	$[0.55; 2.77] \cdot 10^{-6}$	$6.8 \cdot 10^3$
	MCS	$[0.7042; 0.7048]$	$[1.06; 3.2] \cdot 10^{-6}$	10^7

646

647 In the third scenario, hotspots $\{15,16,17,18,19,20\}$ are again inspected in year 10. No fatigue
648 cracks are detected at hotspots $\{15,16,17,18\}$ whereas defects are detected at hotspots $\{19,20\}$.
649 The corresponding posterior annual system failure probabilities are shown for all three dependence
650 cases in Figure 5. The system failure probability increases after the inspection since fatigue cracks
651 are detected in welds connecting two of the most important braces with the legs (see Figure 1 and
652 Table 1). The effect is most pronounced in the low dependence case.

653

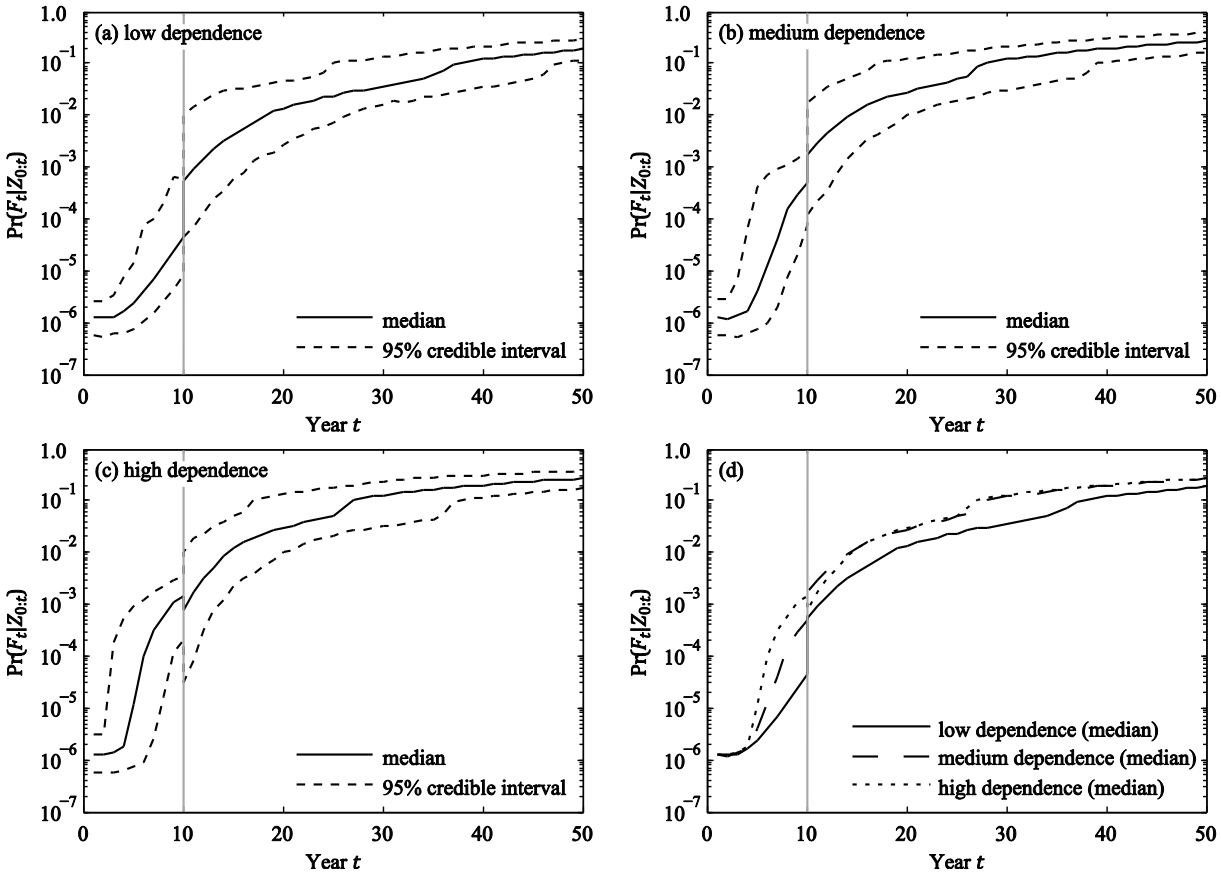

Figure 5. Median and 95% credible interval of the posterior annual system failure probability $\Pr(F_t|Z_{0:t})$ of the Zayas frame as a function of different degrees of dependence among hotspot fatigue behavior. Hotspots {15,16,17,18,19,20} are inspected in year 10. No fatigue cracks are detected at hotspots {15,16,17,18} whereas defects are detected at hotspots {19,20}. Computations are performed with subset simulation as summarized in Section 4 with conditional probabilities $p_0 = 0.1$ and $N = 1000$ samples per subset level. (d) compares the respective medians of the posterior annual system failure probability.

Table 6 shows that the current inspection outcome is approximately two orders of magnitude less probable than the no-detection outcomes in the previous scenarios (see Table 4 and Table 5). When comparing the subset simulation results in Table 5 and Table 6, it can also be seen that the number of model evaluations are similar in both examples although the posterior system failure probabilities $\Pr(F_t|Z_{0:t})$ are multiple orders of magnitude larger in the current example. The reason is that the simulations of the smaller probabilities of the observation event $\Pr(Z_{e,0:t})$ require here more model evaluations.

Table 6. Probability of the inspection outcome $\Pr(Z_{e,0:t})$ and the posterior system failure probability $\Pr(F_t|Z_{0:t})$ at time $t = 10$ years. Subset simulation is performed as summarized in Section 4 with conditional probabilities $p_0 = 0.1$ and $N = 1000$ samples per subset level. Results represent the 95% credible interval. MCS is performed with 10^7 samples. Results represent the 95% confidence interval.

Case	Method	$\Pr(Z_{e,0:t})$	$\Pr(F_t\|Z_{0:t})$	# model runs
Low dependence	SuS	$[2.45; 5.18] \cdot 10^{-3}$	$[0.00429; 1.02] \cdot 10^{-2}$	$7.1 \cdot 10^3$
	MCS	$[3.66; 3.74] \cdot 10^{-3}$	$[2.64; 3.79] \cdot 10^{-3}$	10^7
Medium dependence	SuS	$[2.66; 5.71] \cdot 10^{-3}$	$[0.0121; 1.67] \cdot 10^{-2}$	$6.2 \cdot 10^3$
	MCS	$[3.82; 3.9] \cdot 10^{-3}$	$[6.14; 7.79] \cdot 10^{-3}$	10^7
High dependence	SuS	$[2.57; 5.78] \cdot 10^{-3}$	$[0.0319; 9.84] \cdot 10^{-3}$	$7.0 \cdot 10^3$
	MCS	$[3.86; 3.93] \cdot 10^{-3}$	$[2.96; 4.13] \cdot 10^{-3}$	10^7

In the last scenario, regular inspections are performed at 10 year intervals. Hotspots associated with elements of each importance category are inspected at each inspection apart from the last inspection where only hotspots associated with the upper braces (low importance category) are inspected (see Figure 1 and Table 1). This inspection strategy ensures that each hotspot is inspected at least once throughout the service life of the structure. The inspection strategy is as follows: hotspots $\{15,16,7,8,5,6\}$ are inspected at time $t = 10$ years, hotspots $\{17,18,9,10,13,14\}$ are inspected at time $t = 20$ years, hotspots $\{19,20,11,12,21,22\}$ are inspected at time $t = 30$ years and hotspots $\{1,2,3,4\}$ are inspected at time $t = 40$ years. Each inspection results in a no-detection events. The results are shown in Figure 6. As expected, the positive inspection outcome causes a reduction in the annual system failure probability after each inspection. This effect increases with increasing degree of dependence among hotspot fatigue behavior.

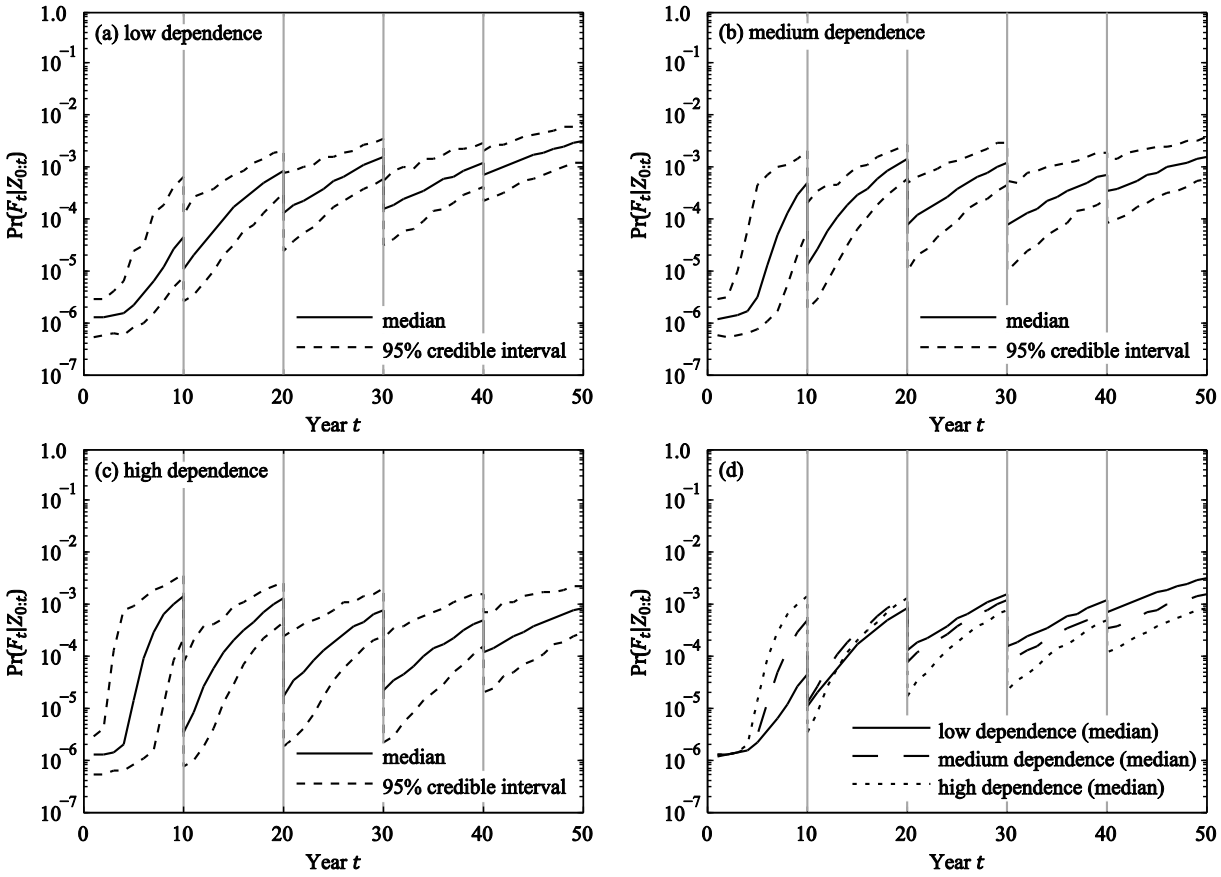

Figure 6. Median and 95% credible interval of the posterior annual system failure probability $\Pr(F_t|Z_{0:t})$ of the Zayas frame as a function of different degrees of dependence among hotspot fatigue behavior. Hotspots {15,16,7,8,5,6} are inspected at time $t = 10$ years, hotspots {17,18,9,10,13,14} are inspected at time $t = 20$ years, hotspots {19,20,11,12,21,22} are inspected at time $t = 30$ years and hotspots {1,2,3,4} are inspected at time $t = 40$ years. No fatigue cracks are detected. Computations are performed with subset simulation as summarized in Section 4 with conditional probabilities $p_0 = 0.1$ and $N = 1000$ samples per subset level. (d) compares the respective medians of the posterior annual system failure probability.

Table 7 summarizes the median probability of the inspection outcome $\Pr(Z_{e,0:t})$ after each inspection. Each additional inspection provides more information on the actual condition of the structure. With increasing amount of information, the probability of the inspection outcome $\Pr(Z_{e,0:t})$ decreases. It also decreases with decreasing degree of dependence among hotspot fatigue behavior.

Table 7. Median of the probability of the inspection outcome $\Pr(Z_{e,0:t})$ as a function of the number of inspections and the degree of dependence among hotspot fatigue behavior.

Year t	low dependence	medium dependence	high dependence
10	0.67	0.69	0.70
20	0.42	0.47	0.52
30	0.25	0.33	0.40
40	0.17	0.26	0.34

6 Application b: Daniels system subjected to fatigue deterioration

We apply the proposed approach to the idealized structural system shown in Figure 7, known as Daniels system (Daniels 1945). We here assume that the Daniels system consists of welded steel members, which are subjected to fatigue deterioration throughout the structure's service life of $T = 50$ years. The properties of the Daniels system, in particular the exchangeability of the elements, facilitate numerical investigations.

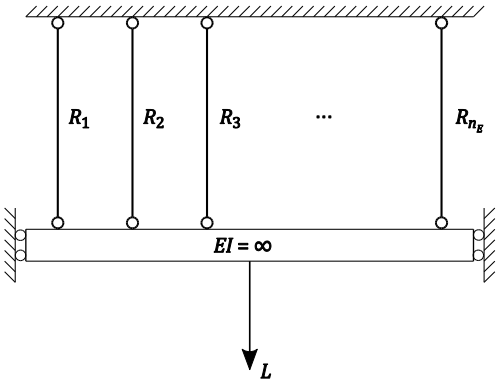

Figure 7. Daniels system with n_E elements.

6.1 System model

The considered Daniels system consists of $n_E = 100$ elements with independent and identically distributed (i.i.d.) capacities R_i, $i = 1, \dots, n_E$. The applied load is shared equally among all elements; its annual maximum is denoted by L. In the current example, we assume that each element is associated with one welded connection. Furthermore, we assume that each welded connection contains only one critical hotspot, i.e. $n_H = n_E = 100$.

The same deterioration model presented in Section 5 is applied to model fatigue deterioration of the Daniels system. At any time t there are $N_{F,t}$ failed elements and $n_E - N_{F,t}$ elements are available to resist the applied loads. Because of the exchangeability of its elements, $N_{F,t}$ represents the deterioration state of the Daniels system at time t. $N_{F,t}$ is computed as a function h of the deterioration model parameters $\mathbf{X}$ as:

$$N_{F,t} = h(\mathbf{X}, t) = \sum_{i=1}^{n_E} I(g_i(\mathbf{X}, t) \leq 0) \tag{59}$$

where $g_i(\mathbf{X}, t)$ is the limit-state function defining the event of fatigue failure of element i; see Equation (44). The system failure probability of the Daniels system in the reference period $[t - \Delta t, t]$ conditional on a realization of the fatigue model parameters $\mathbf{X} = \mathbf{x}$ can now be written as:

$$p_F(\mathbf{x}, t) = \Pr\left(F_t | N_{F,t} = h(\mathbf{x}, t)\right) \tag{60}$$

For given probability distributions of the component capacities R_i and the annual maximum load L, the conditional system failure probability $\Pr(F_t | N_{F,t} = k)$, $k = 0, \dots, n_E$ is readily determined from Daniels system formulation. This failure probability has a reference period $\Delta t = 1$ year but it is independent of time t. For ductile element behavior (steel elements), the solution is given by (Gollwitzer and Rackwitz 1990):

$$\Pr(F_t | N_{F,t} = k) = \Pr\left(\sum_{i=1}^{n_E - k} R_i \leq L\right) \tag{61}$$

The right hand side of Equation (61) corresponds to a component reliability problem, which can be solved using structural reliability methods.

In the current example, the component capacities R_i, $i = 1, \dots, n_E$ are modeled as i.i.d. normal random variables with c.o.v. $\delta_R = 0.15$. The annual maximum of the applied load L is modeled as a lognormal random variable with c.o.v. $\delta_L = 0.25$. The ratio of the mean values of $n_E R_i$ and L is selected such that the undamaged Daniels system has a probability of failure $\Pr(F_t | N_{F,t} = 0) = 1.3 \times 10^{-6}$. The resulting ratio is $n_E \mu_{R_i} / \mu_L = 3.09$. $\Pr(F_t | N_{F,t} = k)$, $k = 0, \dots, n_E$ is pre-calculated for each realization of the system deterioration state by solving Equation (61) using the first-order reliability method (FORM). The results are illustrated in Figure 8. In the subsequent reliability analysis of the deteriorating Daniels system, the computation of $p_F(\mathbf{x}, t)$ is again reduced to a lookup operation.

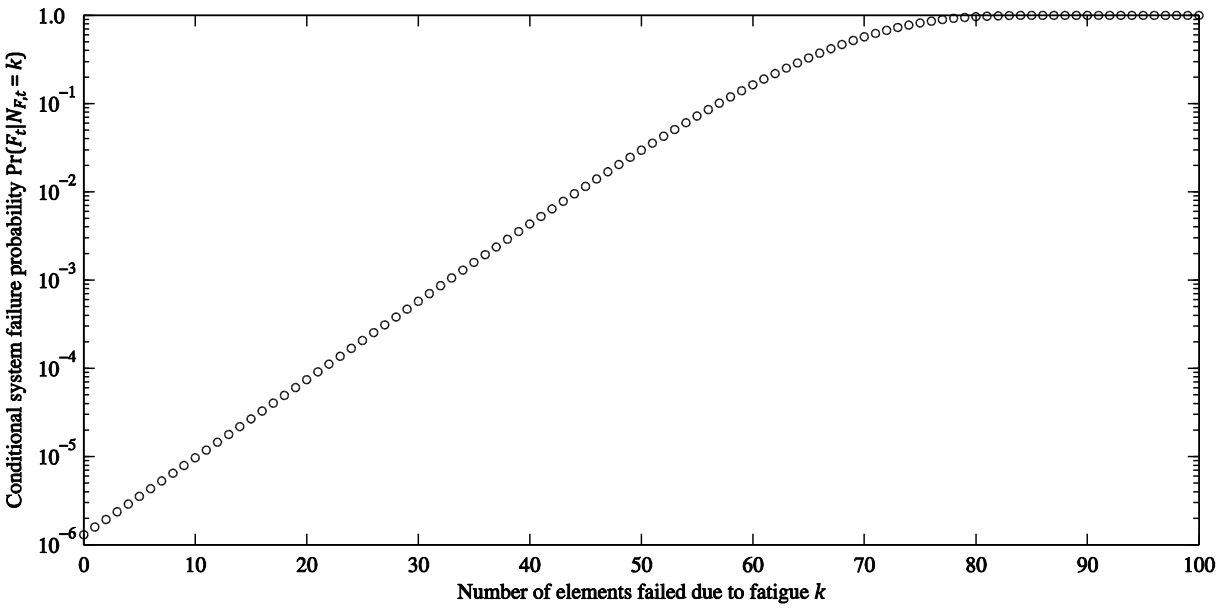

735 Figure 8. Failure probability of the Daniels system as a function of the number of elements failed due to
736 fatigue.

737 Each element of the Daniels system is equally important due to the perfect load sharing among the
738 structural elements. The single element importance measure of an individual element i of the
739 Daniels system is $\mathrm{SEI}_i = \Pr(F_t|N_{F,t} = 1) - \Pr(F_t|N_{F,t} = 0) = 2.9 \times 10^{-7}$. The Daniels system
740 is highly redundant with respect to single element failure when compared to the Zayas frame
741 studied in Section 5 where failure of elements of the highest importance category lead to a
742 significant reduction in system reliability, see Table 1.

743 ## 6.2 Prior system reliability analysis

744 The computed prior annual system failure probability $\Pr(F_t)$ of the Daniels system is shown in
745 Figure 9 for each degree of dependence among hotspot fatigue. Computations are performed with
746 subset simulation as summarized in Section 4 with conditional probabilities $p_0 = 0.1$ and $N =$
747 1000 samples per subset level.

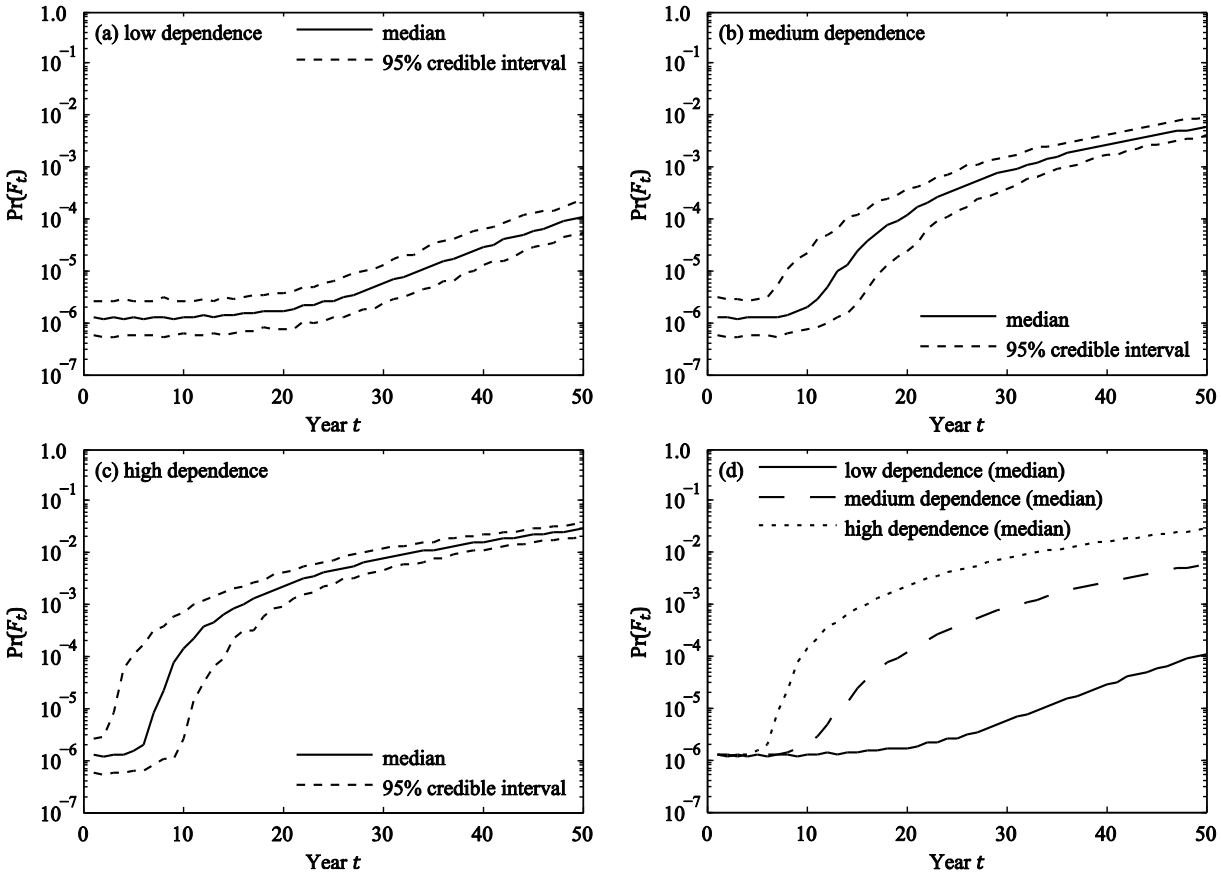

Figure 9. Median and 95% credible interval of the prior annual system failure probability $\Pr(F_t)$ of the Daniels system as a function of different degrees of dependence among hotspot fatigue behavior. Computations are performed with subset simulation as summarized in Section 4 with conditional probabilities $p_0 = 0.1$ and $N = 1000$ samples per subset level. (d) compares the respective medians of the prior annual system failure probability.

In general, a large dependence among element deterioration behavior increases the probability of joint occurrence of more than one element deterioration failures. Figure 9 shows that this behavior has a significant influence on the reliability of the Daniels system. This outcome is expected for a structural system with a large redundancy. In contrast, the results computed for the Zayas frame show that the influence of correlation among element deterioration failures is less pronounced for structural systems with limited or no redundancy (see Figure 2).

6.3 Posterior system reliability analysis

To study the effect of inspections on the reliability of the Daniels system, different inspection scenarios in terms of inspection times and coverage are considered. Each inspection is assumed to result in a no detection event. The same inspection model as presented in Section 5.3 is applied.

In the first scenario, hotspots $\{1 \text{ to } 10\}$ are inspected at time $t = 10$ years. The updated annual system failure probabilities $\Pr(F_t|Z_{0:t})$ of the Daniels system are shown in Figure 10 for each degree of dependence among hotspot fatigue behavior. In all three dependence cases, the system

failure probability decreases after the inspection due to the positive inspection outcome. After the inspection, the system failure probability is reduced to its lower limit, which corresponds to the reliability of the undamaged structure at the beginning of its service live. The subsequent increase in the annual system failure probability is most pronounced in the high-dependence case.

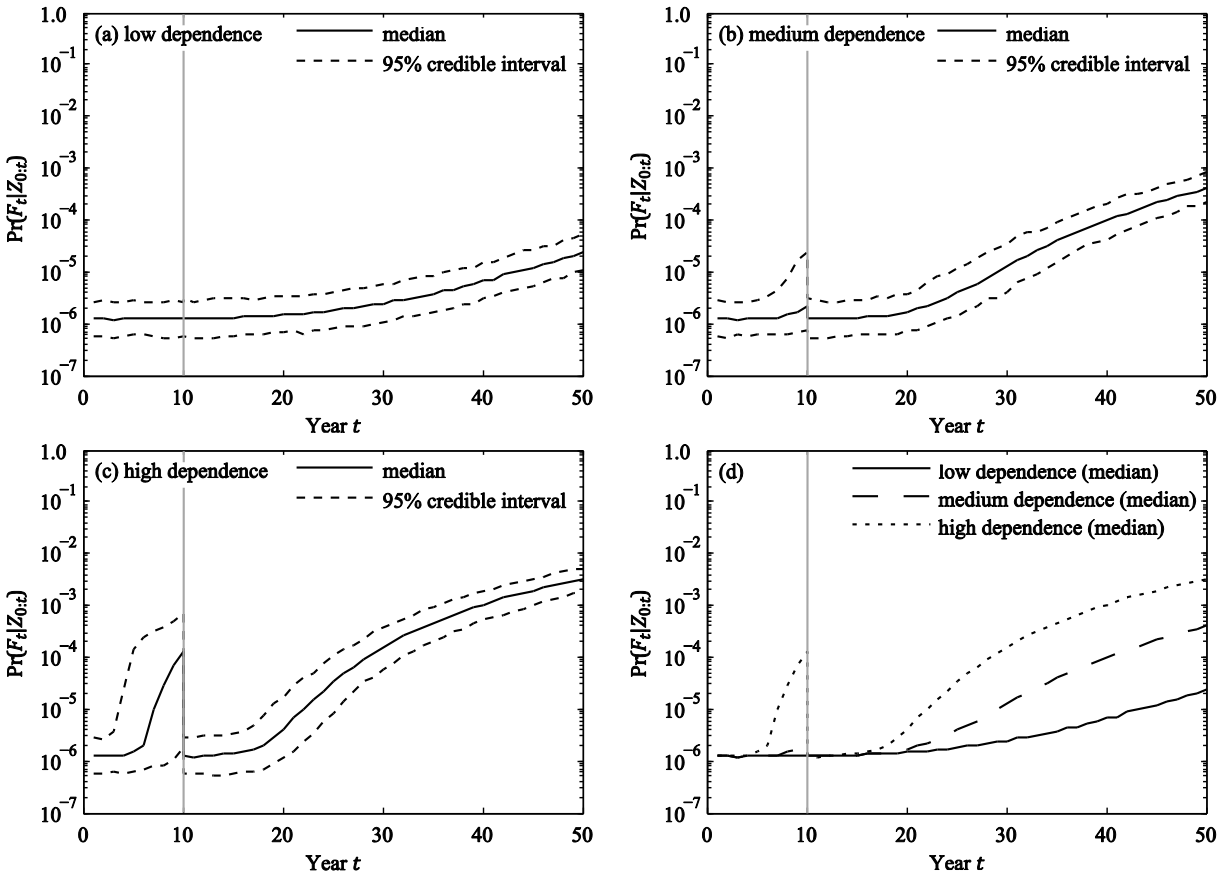

Figure 10. Median and 95% credible interval of the posterior annual system failure probability $\Pr(F_t|Z_{0:t})$ of the Daniels system as a function of different degrees of dependence among hotspot fatigue behavior. hotspots {1 to 10} are inspected in year 10. No fatigue cracks are detected. Computations are performed with subset simulation as summarized in Section 4 with conditional probabilities $p_0 = 0.1$ and $N = 1000$ samples per subset level. (d) compares the respective medians of the posterior annual system failure probability.

In the second scenario, different sets of hotspots are inspected at 10 year intervals. The inspection strategy is as follows: hotspots {1 to 10} are inspected at time $t = 10$ years, hotspots {11 to 20} are inspected at time $t = 20$ years, hotspots {21 to 30} are inspected at time $t = 30$ years and hotspots {31 to 40} are inspected at time $t = 40$ years. The results are shown in Figure 11. In all three dependence cases, the posterior annual system failure probability is close the annual failure probability of the undamaged structures after all inspections are performed.

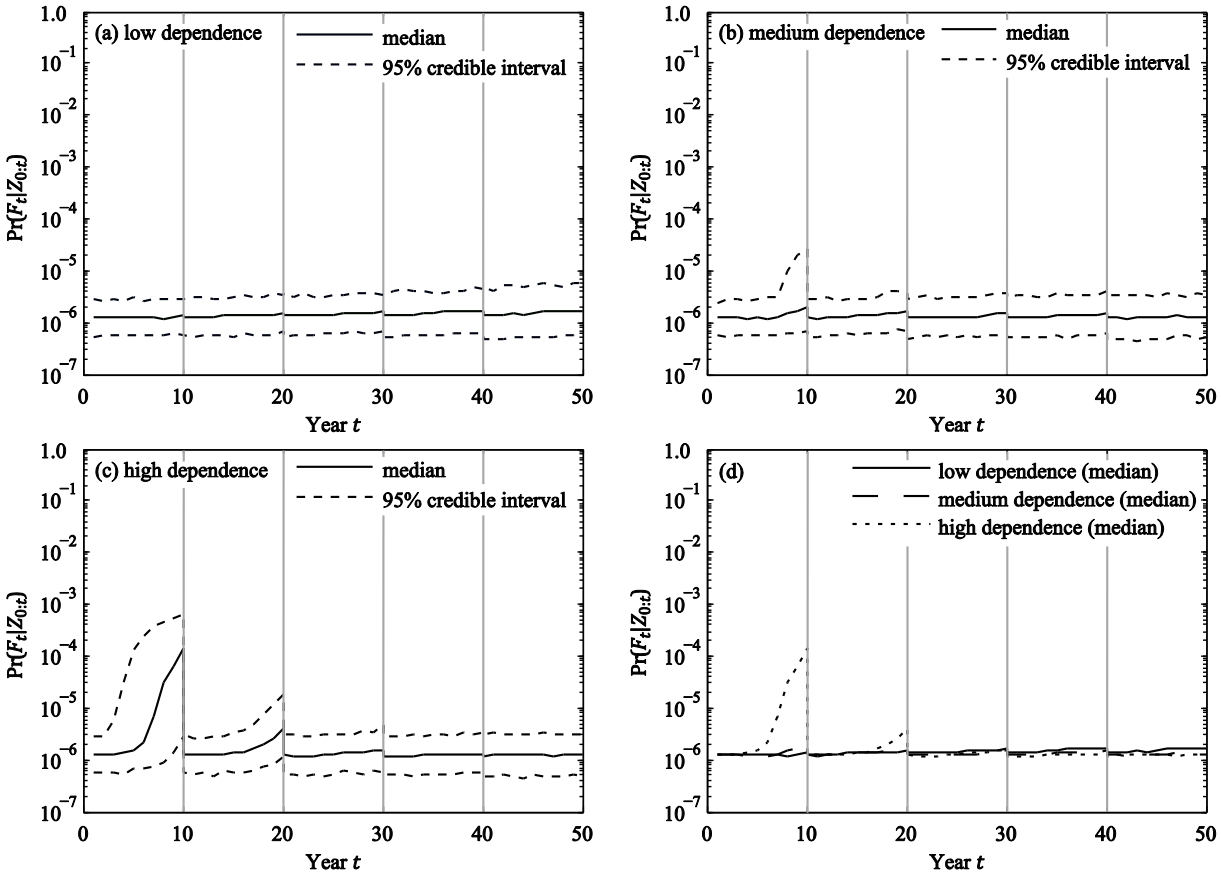

Figure 11. Median and 95% credible interval of the posterior annual system failure probability $\Pr(F_t|Z_{0:t})$ of the Daniels system as a function of different degrees of dependence among hotspot fatigue behavior. Hotspots {1 to 10} are inspected at time $t = 10$ years, hotspots {11 to 20} are inspected at time $t = 20$ years, hotspots {21 to 30} are inspected at time $t = 30$ years and hotspots {31 to 40} are inspected at time 40 years. Each inspection results in a no-detection event. Computations are performed with subset simulation as summarized in Section 4 with conditional probabilities $p_0 = 0.1$ and $N = 1000$ samples per subset level. (d) compares the respective medians of the posterior annual system failure probability.

7 Discussion

We propose a modeling and computational framework for analyzing the reliability of deteriorating structural systems and updating it with inspection and monitoring data. It enables an integral assessment of deterioration at the element level together with the structural system performance and structural condition information. The interdependences among the element deterioration states are included. Only few previous works have addressed such an integral system analysis (e.g. Lee and Song 2014; Schneider et al. 2015; Luque and Straub 2016). In contrast to these approaches, the main advantage of the proposed framework is the fact that it can be implemented easily through the use of subset simulation. It is computationally robust since it provides reasonably accurate solutions without a need for tailoring the algorithm to specific applications. It is also computationally efficient for many applications, as discussed further below.

The results in the paper demonstrate the importance of considering dependence among element deterioration when evaluating the structural system reliability. For the considered redundant systems, the dependence leads to a decrease in the prior (unconditional) system reliability. This effect is more pronounced as the system redundancy increases (from the Zayas frame to the Daniels system). When including inspection results, dependence among element deterioration means that the state of non-inspected elements can be inferred from the inspection results. As long as inspections do not indicate serious problems, this additional learning leads to a reduction of uncertainty and hence to an increase in the overall system reliability. In the considered case studies, the posterior (conditional) reliability after the inspections is fairly similar for the different degrees of dependence. However, this is not expected to occur if inspections do indicate larger damage.

The framework can handle any type of information on the deterioration state of the structure, as long as a corresponding likelihood function is formulated. In particular, the framework can also include information from monitoring systems. For monitoring systems, which provide potentially large amount of data, it might be beneficial to pre-process the data. In such a pre-processing step (e.g. a system identification), the probability of the observed data given the deterioration states of the structure is determined. This probability is the likelihood function that is inputted into Equations (34) and (35). Such an approach is similar to a two-stage Bayesian analysis for system identification (see Au and Zhang 2015).

The use of subset simulation is computationally rather efficient, as demonstrated in the case studies. Here, no attempt was made to optimize the efficiency of subset simulation. The number of samples per subset level was chosen such that the results have a reasonable accuracy. Their accuracies can always be improved or reduced by increasing or decreasing the number of samples per subset level. It should be noted, however, that the number of required subsets increases with increasing amount of information, i.e. with decreasing $\Pr(Z_{e,0:t})$.

The proposed framework relies on the separation of the computation of the system deterioration state $\mathbf{D}_t$ and structural system reliability conditional on $\mathbf{D}_t = \mathbf{d}_t$. Here, two situations must be distinguished: Applications, in which the conditional probability $\Pr(F_t|\mathbf{D}_t = \mathbf{d}_t)$ can be pre-computed, and those in which it cannot. The former occurs if the numbers of distinct states in $\mathbf{D}_t$ is limited. If the structural system reliability analysis is demanding, it might take some computation time for establishing a database with all values of $\Pr(F_t|\mathbf{D}_t = \mathbf{d}_t)$, but this is typically not critical, as this computation must be carried out only once and the database can be used for all subsequent reliability updating calculations. If the number of states in $\mathbf{D}_t$ is too large to enable pre-computation, because there are too many elements or because continuous damage states are considered, $\Pr(F_t|\mathbf{D}_t = \mathbf{d}_t)$ must be computed on the fly. If such calculations are inexpensive (e.g. through a FORM analysis), the separation of the system deterioration state and structural system reliability is still computationally beneficial. In cases where pre-computation of $\Pr(F_t|\mathbf{D}_t = \mathbf{d}_t)$ is not an option, and in which it is expensive to compute it on the fly, there are two possible strategies: (a) One can investigate the possibility of developing a response surface for

838 $\Pr(F_t|\mathbf{D}_t = \mathbf{d}_t)$. Since $\mathbf{D}_t$ is typically discrete, many of the classical response surface techniques
839 used in structural reliability will not be suitable. This is an area of future research. (b) Alternatively,
840 the proposed framework can be modified to solve the system deterioration updating and the system
841 reliability jointly. In this case, however, the advantages of the de-coupling are lost.

842 Potentials for further developments are seen in integrating the presented method into the
843 framework of pre-posterior decision analysis to identify optimal inspection, monitoring and
844 maintenance strategies for engineering structures (e.g. Straub and Faber 2005; Thöns and Faber
845 2013; Straub 2014).

846 # 8 Conclusions

847 We propose a novel approach to modeling and analyzing the system reliability of deteriorating
848 structural systems in conjunction with structural condition information, which considers stochastic
849 interdependence among the deterioration states of the structural elements. The approach provides
850 the means to consistently utilize inspection and monitoring information on the deterioration state
851 of structures to update the system failure probability. Through the application of subset simulation,
852 the approach can be implemented relatively easily and is considerably more efficient than crude
853 Monte Carlo simulation.

854

855 # Acknowledgements

856 We acknowledge insightful discussions with Iason Papaioannou and Wolfgang Betz on the
857 implementation of the adaptive MCMC sampling algorithm. The work of Daniel Straub is
858 supported by the German Science Foundation (DFG) through Grant STR 1140/3-1.

859

860 # References

861 Altamura, A. and D. Straub (2014). "Reliability assessment of high cycle fatigue under variable
862 amplitude loading: review and solutions." Engineering Fracture Mechanics **121**: 40-66.

863 Au, S.-K. and J. L. Beck (2001). "Estimation of small failure probabilities in high dimensions by
864 subset simulation." Probabilistic Engineering Mechanics **16**(4): 263-277.

865 Au, S.-K., F. A. DiazDelaO and I. Yoshida (2015). "Bayesian updating and model class selection
866 with Subset Simulation." eprint arXiv:1510.06989.

867 Au, S.-K. and F.-L. Zhang (2015). "Fundamental two-stage formulation for Bayesian system
868 identification, Part I: General theory." Mechanical Systems and Signal Processing.

869 Betz, W., I. Papaioannou and D. Straub (2014a). "Numerical methods for the discretization of
870 random fields by means of the Karhunen–Loève expansion." Computer Methods in
871 Applied Mechanics and Engineering **271**: 109–129.

872 Betz, W., I. Papaioannou and D. Straub (2014b). Adaptive variant of the BUS approach to Bayesian
873 updating. 9th International Conference on Structural Dynamics (EURODYN 2014). Porto,
874 Portugal.

875 Ciampoli, M. (1998). "Time dependent reliability of structural systems subject to deterioration."
876 Computers & Structures **67**(1–3): 29-35.

877 Daniels, H. E. (1945). "The statistical theory of the strength of bundles of threads. I." Proceedings
878 of the Royal Society of London: 405-435.

879 Ditlevsen, O. and P. Bjerager (1986). "Methods of structural systems reliability." Structural Safety
880 **3**(3): 195-229.

881 Ditlevsen, O. and H. O. Madsen (1996). Structural Reliability Methods, John Wiley & Sons Ltd.

882 Enright, M. P. and D. M. Frangopol (1999). "Condition prediction of deteriorating concrete bridges
883 using Bayesian updating." Journal of Structural Engineering **125**(10): 1118-1125.

884 Estes, A. and D. Frangopol (1999). "Repair Optimization of Highway Bridges Using System
885 Reliability Approach." Journal of Structural Engineering **125**(7): 766-775.

886 Faber, M. H., S. Engelund, J. D. Sørensen and A. Bloch (2000). Simplified and Generic Risk Based
887 Inspection Planning. 19th Conference on Offshore Mechanics and Arctic Engineering
888 (OMAE), New Orleans, Louisiana, USA.

889 Faber, M. H., D. Straub and M. A. Maes (2006). "A computational framework for risk assessment
890 of RC structures using indicators." Computer-Aided Civil and Infrastructure Engineering
891 **21**(3): 216-230.

892 Fricke, W. (2003). "Fatigue analysis of welded joints: state of development." Marine Structures
893 **16**(3): 185-200.

894 Gollwitzer, S. and R. Rackwitz (1990). "On the reliability of Daniels systems." Structural Safety
895 **7**(2-4): 229–243.

896 Gurney, T. R. (1978). An analysis of some recent fatigue crack propagation data for steels subjected
897 to pulsating tension loading. Report 1978E, The Welding Institute TWI, UK

898 Hergenröder, M. (1992). Zur statistischen Instandhaltungsplanung für bestehende Betonbauwerke
899 bei Karbonatisierung des Betons und möglicher Korrosion der Bewehrung PhD,
900 Technische Universität München.

901 Hohenbichler, M. and R. Rackwitz (1981). "Non-Normal Dependent Vectors in Structural Safety."
902 Journal of the Engineering Mechanics Division **107**(6): 1227-1238.

903 Hohenbichler, M. and R. Rackwitz (1983). "First-order concepts in system reliability." Structural
904 Safety **1**(3): 177-188.

905 Lee, Y.-J. and J. Song (2014). "System Reliability Updating of Fatigue-Induced Sequential
906 Failures." Journal of Structural Engineering **140**(3).

907 Li, C. Q. (1995). "Computation of the failure probability of deteriorating structural systems."
908 Computers & Structures **56**(6): 1073-1079.

909 Li, Q., C. Wang and B. R. Ellingwood (2015). "Time-dependent reliability of aging structures in
910 the presence of non-stationary loads and degradation." Structural Safety **52, Part A**: 132-
911 141.

912 Li, Y., T. Vrouwenvelder, G. H. Wijnants and J. Walraven (2004). "Spatial variability of concrete
913 deterioration and repair strategies." Structural Concrete **5**(3): 121-129.

914 Lin, Y. K. and J. N. Yang (1985). "A stochastic theory of fatigue crack propagation." AIAA Journal
915 **23**(1): 117-124.

916 Liu, P.-L. and A. Der Kiureghian (1986). "Multivariate distribution models with prescribed
917 marginals and covariances." Probabilistic Engineering Mechanics **1**(2): 105-112.

918 Luque, J., R. Hamann and D. Straub (2016). "Spatial probabilistic modeling of corrosion in ships
919 structures." ASCE-ASME Journal of Risk and Uncertainty in Engineering Systems, Part
920 B: Mechanical Engineering: submitted.

921 Luque, J. and D. Straub (2016). "Reliability analysis and updating of deteriorating systems with
922 dynamic Bayesian networks." Structural Safety **62**: 34-46.

923 Madsen, H. O. (1987). Model updating in reliability theory. 5th International Conference on
924 Applications of Statistics and Probability in Civil Engineering (ICASP 5). Vancouver,
925 Canada.

926 Madsen, H. O. (1997). Stochastic modeling of fatigue crack growth and inspection. Probabilistic
927 Methods for Structural Design. C. Guedes Soares, Kluwer Accademic Publishers,
928 Netherlands.

929 Madsen, H. O., S. Krenk and N. C. Lind (1986). Methods of Structural Safety, Prentice Hall.

930 Maes, M. A. and M. Dann (2007). "Hierarchical Bayes methods for systems with spatially varying
931 condition states." Canadian Journal of Civil Engineering **34**(10): 1289-1298.

932 Malioka, V. (2009). Condition Indicators for the Assessment of Local and Spatial Deterioration of
933 Concrete Structures. PhD, ETH Zurich.

934 Maljaars, J. and A. C. W. M. Vrouwenvelder (2014). "Probabilistic fatigue life updating accounting
935 for inspections of multiple critical locations." International Journal of Fatigue **68**: 24-37.

936 Melchers, R. E. (1999a). "Corrosion uncertainty modelling for steel structures." Journal of
937 Constructional Steel Research **52**(1): 3-19.

938 Melchers, R. E. (1999b). Structural Reliability Analysis and Prediction, John Wiley and Sons Ltd.

939 Moan, T. (2005). "Reliability-based management of inspection, maintenance and repair of offshore
940 structures." Structure and Infrastructure Engineering **1**(1): 33-62.

941 Moan, T. and R. Song (2000). "Implications of Inspection Updating on System Fatigue Reliability
942 of Offshore Structures." Journal of Offshore Mechanics and Arctic Engineering **122**(3):
943 173-180.

944 Moan, T., O. T. Vardal, N. C. Hellevig and K. Skjoldli (2000). "Initial crack depth and PoD values
945 inferred from in-service observations of cracks in North Sea jackets." Journal of Offshore
946 Mechanics and Arctic Engineering **122**: 157-162.

947 Mori, Y. and B. Ellingwood (1993). "Reliability-Based Service-Life Assessment of Aging
948 Concrete Structures." Journal of Structural Engineering **119**(5): 1600-1621.

949 Naess, A., B. J. Leira and O. Batsevych (2009). "System reliability analysis by enhanced Monte
950 Carlo simulation." Structural Safety **31**(5): 349-355.

951 Papaioannou, I., W. Betz, K. Zwirgelmaier and D. Straub (2015). "MCMC Algorithms for Subset
952 Simulation." Probabilistic Engineering Mechanics **41**: 89-103.

953 Paris, P. C. and F. A. Erdogan (1963). "A critical analysis of crack propagation laws." Journal of
954 Basic Engineering **85**: 528-534.

955 Qin, J. and M. H. Faber (2012). "Risk Management of Large RC Structures within a Spatial
956 Information System." Computer-Aided Civil and Infrastructure Engineering **27**: 385–405.

957 Schneider, R., J. Fischer, M. Bügler, M. Nowak, S. Thöns, A. Borrmann and D. Straub (2015).
958 "Assessing and updating the reliability of concrete bridges subjected to spatial deterioration
959 - principles and software implementation." Structural Concrete **16**(3): 356–365.

960 Schneider, R., S. Thöns, W. Rücker and D. Straub (2013). Effect of different inspection strategies
961 on the reliability of Daniels systems subjected to fatigue. 11th International Conference on
962 Structural Safety & Reliability (ICOSSAR 2013). New York, USA.

963 Schuëller, G. I. and H. J. Pradlwarter (2007). "Benchmark study on reliability estimation in higher
964 dimensions of structural systems – An overview." Structural Safety **29**(3): 167-182.

965 Skallerud, B. and J. Amdahl (2002). Nonlinear analysis of offshore structures. UK, Reasearch
966 Studies Press Ltd.

967 Song, J. and W.-H. Kang (2009). "System reliability and sensitivity under statistical dependence
968 by matrix-based system reliability method." Structural Safety **31**(2): 148–156.

969 Stewart, M. and D. Val (1999). "Role of Load History in Reliability-Based Decision Analysis of
970 Aging Bridges." Journal of Structural Engineering **125**(7): 776-783.

971 Stewart, M. G. and J. A. Mullard (2007). "Spatial time-dependent reliability analysis of corrosion
972 damage and the timing of first repair for RC structures." Engineering Structures **29**(7):
973 1457-1464.

974 Straub, D. (2004). Generic Approaches to Risk Based Inspection Planning for Steel Structures,
975 ETH Zürich.

976 Straub, D. (2011a). "Reliability updating with equality information." Probabilistic Engineering
977 Mechanics **26**(2): 254–258.

978 Straub, D. (2011b). Reliability updating with inspection and monitoring data in deteriorating
979 reinforced concrete slabs. 11th International Conference on Applications of Statistics and
980 Probability in Civil Engineering. Zurich, Switzerland.

981 Straub, D. (2014). "Value of Information Analysis with Structural Reliability Methods." Structural
982 Safety **49**: 75-85.

983 Straub, D. and A. Der Kiureghian (2010). "Bayesian network enhanced with structural reliability
984 methods: Methodology." Journal of Engineering Mechanics **136**(10): 1248-1258.

985 Straub, D. and A. Der Kiureghian (2011). "Reliability acceptance criteria for deteriorating
986 elements of structural systems." Journal of Structural Engineering **137**(12): 1573-1582.

987 Straub, D. and M. H. Faber (2003). Modeling Dependency in Inspection Performance. 9th
988 International Conference on Applications of Statistics and Probability in Civil Engineering.
989 San Francisco, California.

990 Straub, D. and M. H. Faber (2005). "Risk based inspection planning for structural systems."
991 Structural Safety **27**: 335–355.

992 Straub, D. and M. H. Faber (2007). "Temporal Variability in Corrosion Modeling and Reliability
993 Updating." Journal of Offshore Mechanics and Arctic Engineering **129**(4): 265-272.

994 Straub, D. and I. Papaioannou (2015a). Bayesian analysis for learning and updating geotechnical
995 parameters and models with measurements. Risk and reliability in geotechnical
996 engineering. K.-K. Phoon and J. Ching, CRC Press.

997 Straub, D. and I. Papaioannou (2015b). "Bayesian updating with structural reliability methods."
998 Journal of Engineering Mechanics **141**(3).

999 Straub, D., I. Papaioannou and W. Betz (2016). "Bayesian analysis of rare events." Journal of
1000 Computational Physics: accepted.

1001 Tang, W. H. (1973). "Probabilistic updating of flaw information." Journal of Testing and
1002 Evaluation **1**(6): 459-467.

1003 Thoft-Christensen, P. and Y. Murotsu (1986). Application of Structural Systems Reliability Theory,
1004 Springer-Verlag.

1005 Thoft-Christensen, P. and J. D. Sørensen (1987). "Optimal strategy for inspection and repair of
1006 structural systems." Civil Engineering Systems **4**: 94-100.

1007 Thöns, S. and M. H. Faber (2013). Assessing the Value of Structural Health Monitoring. 11th
1008 International Conference on Structural Safety & Reliability (ICOSSAR 2013). New York,
1009 USA.

1010 Ultiguide (1999). Best practice guidelines for use of non-linear methods in documentation of
1011 ultimate limit states for jacket type offshore structures, Det Norske Veritas (DNV), Norway

1012 USFOS (2014). Ultimate Strength of Framed Offshore Structures. Version 8-7, USFOS A/S,
1013 Norway

1014 Vrouwenvelder, A. C. W. M. (2004). Spatial correlation aspects in deterioration models. 2nd
1015 International Conference on Lifetime-Oriented Design Concepts. Bochum, Germany.

1016 Wen, Y. K. and H.-C. Chen (1987). "On fast integration for time variant structural reliability."
1017 Probabilistic Engineering Mechanics **2**(3): 156-162.

Zayas, V. A., S. A. Mahin and E. P. Popov (1980). Cyclic inelastic behavior of steel offshore structures. UCB/EERC-80/27, University of California, Berkley, USA